Chapter 2
Conductive Nanostructured Scaffolds for Guiding Tissue Regeneration

Haiyan Xu, Jie Meng, and Tao Wen

Abstract Biological electricity is ubiquitous in life to maintain many functions of organs. Therefore, conductivity is one crucial factor to biomaterial scaffolds guiding electrically excitable tissue regeneration. Accumulating evidence has indicated the importance of providing electrical active microenvironments mimicking natural physiological conditions. In this chapter, various kinds of conductive scaffolds and processing technologies are introduced, and application potentials of the conductive scaffolds are revealed by typical examples of guiding different tissue regeneration include cardiac, skeletal, nerve, and skin. In addition, synergistic effects of conductivity and mechanical property of tissue engineering scaffolds are addressed as well, and underling mechanisms have been explored and discussed.

Keywords Conductive · Scaffolds · Tissue regeneration · Nanoparticles · Nanostructures

2.1 Introduction

Biological electricity is ubiquitous in life; for example, excitable tissues such as heart and nerve have closer relationship with electricity, and bone and skin are reported having electromagnetic activity as well [1]. These tissues can rapidly change electrochemical impulses at the cell membranes to transmit signals along the muscle membranes or nerves, maintaining the functions of the organs. For example, heart is composed of three major types of cardiac muscle including atrial muscle, ventricular muscle, and specialized excitatory and conductive muscle fibers that play vital roles in the electrical signal transduction. The cardiac muscle generates action potentials passing over the cardiac muscle membrane and spreading to the interior of the cardiac

H. Xu (✉) · J. Meng · T. Wen
Department of Biomedical Engineering, Institute of Basic Medical Sciences, Chinese Academy of Medical Sciences and Peking Union Medical College, Beijing, P. R. China
e-mail: xuhy@pumc.edu.cn

H. Xu, N. Gu (eds.), *Nanotechnology in Regenerative Medicine and Drug Delivery Therapy*, https://doi.org/10.1007/978-981-15-5386-8_2

muscle fiber along the membranes of the transverse tubules and then the membranes of the longitudinal sarcoplasmic tubules to cause release of calcium ions into the muscle sarcoplasm from the sarcoplasmic reticulum. These calcium ions diffuse into the myofibrils and catalyze the chemical reactions that promote sliding of the actin and myosin filaments along one another, which produces muscle contraction. Therefore, the normal functions of excitable tissues rely on the electrical signal transduction between the cells. This nature can explain why conductive scaffolds have attracted intense research interests on tissue regeneration. Experimental evidence is increasing that conductive scaffolds can promote adhesion, proliferation, migration, and differentiation of cells, including cardiac, nerve, bone, muscle, fibroblasts, keratinocytes, and mesenchymal stem cells. In this chapter, conductive scaffolds are introduced from design and fabrication, electrical and mechanical properties, and the interactions between the scaffolds and tissue specific cells as well as stem cells, mainly including cardiomyocytes, neuron cells, skeletal cells, bone related cells, and fibroblasts, and their therapeutic effects on the tissue regeneration.

2.2 Classification and Fabrication of Conductive Scaffolds

Conductive scaffolds can be in general summarized to two main categories according the conductive substances included in scaffolds (Fig. 2.1), one kind of additives is conductive polymers such as polypyrrole (PPY) and polyaniline (PANi), and the other one is conductive nanoparticles such as carbon nanotubes, graphene, gold nanoparticles, and silica wire. From the view of structures, nanostructures are highly involved in the fabrication of conductive scaffolds; hence, the two categories can be further divided into subclasses, including nanocomposite hydrogels and scaffolds with nanofibrous, nano-roughness, micro–nano-patterned structures, and casting or molding scaffolds with embedded nanomaterials, all of which are intended to mimic the structural features of natural extracellular matrix where cells live in.

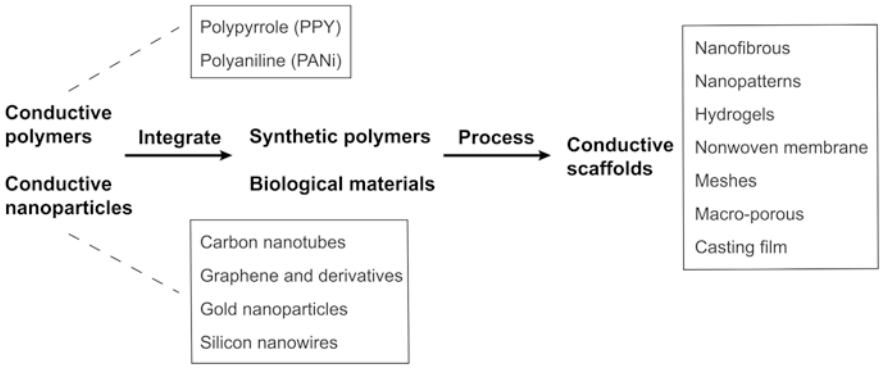

Fig. 2.1 Summary of conductive materials and scaffolds for tissue engineering and regenerative medicine

2.2.1 Conductive Polymers

Conductive polymers are organic electronically conjugated polymers with electro-optic properties like those of metals, which is one important class of the candidates as conductive components to give scaffolds conductivity. The polymers can form electrical pathways of charge carriers because π-electrons move freely within the molecular chain [2, 3]. Polymers with intrinsic conductive properties have been largely studied in relation to their incorporation into various scaffolds for uses in tissue engineering and regeneration. The reason for this interest is that such scaffolds could electrically stimulate cells and thus regulate specific cellular activities and by this means influence the process of regeneration of those tissues that respond to electrical impulses.

There are several kinds of conductive polymers that have been reported in literatures, mostly investigated in tissue engineering and regenerative medicine are polypyrrole (PPY) and polyaniline (PANi). The two macromolecules possess the good conductivity of 10^2~5×10^3 and 10–10^7 S/m, respectively [3]. For comparison, the range of conductivity of ventricular muscle, blood, and skeletal muscle is 0.03–0.6 S/m [4]. However, disadvantages of mechanical properties and biocompatibility for these polymers are obvious as well. For examples, PPY is insoluble in water, susceptible to irreversible oxidation, and fragile; and PANi has low solubility in aqueous solution, lack of plasticity, and poor cell adhesion and growth. Therefore, it is no surprise that the two conductive polymers are usually used in combination with other materials to develop conducting composite scaffolds for tissue engineering and regenerative medicine.

2.2.2 Conductive Inorganic Nanoparticles

Some kinds of nanoparticles are electrically conductive, mainly including graphene, carbon nanotubes, gold nanoparticles, silver nanoparticles, and silica nanowire, which have been investigated in the tissue engineering and regenerative medicine. Below is a brief introduction about the conductive nanoparticles.

Graphene is strictly a two-dimensional (2D) material that exhibits exceptionally high crystal and electronic quality, rapidly rising on the horizon of materials science and physics, and has already revealed a cornucopia of new physics and potential applications [5]. The 2D carbon nanomaterials commonly include three kinds of graphene: graphene oxide (GO), a highly oxidative form of graphene, reduced graphene oxide (rGO), and graphene sheets [6]. There are several methods to synthesize graphene, commonly classified to four different methods including chemical vapor deposition and epitaxial growth, micromechanical exfoliation, epitaxial growth on electrically insulating surfaces, and the creation from colloidal suspensions [7]. Graphene is a giant aromatic macromolecule that conducts both electricity and heat well in two dimensions. It has a large theoretical specific surface area

(2630 m^2/g), high intrinsic mobility (200,000 cm^2/v s), high Young's modulus (~1.0 TPa) and thermal conductivity (~5000 W/m K), good optical transmittance (~97.7%), and good electrical conductivity [8]. These fascinating properties of GOs are mainly derived from its unique chemical structures composed of small sp^2 carbon domains surrounded by sp^3 carbon domains and oxygen containing hydrophilic functional groups [6]. The graphene is honeycomb lattice, which is composed of two equivalent sub-lattices of carbon atoms bonded together with σ-bonds. Each carbon atom in the lattice has a π orbital that contributes to a delocalized network of electrons. This atomic structure, combined with the electron distribution of graphene, results in high electrical conductivity. Electrons in graphene, obeying a linear dispersion relation, behave like massless relativistic particles [9]. Chemically functionalized graphene can be readily mixed with other polymers in solution, producing a new class of electrically conductive nanocomposites [10].

Carbon nanotubes are unique tubular structures of nanometer diameter and large length/diameter ratio. There are two main types of carbon nanotubes: single-walled carbon nanotubes (SWNTs) and multi-walled carbon nanotubes (MWNTs). SWNTs consist of a single graphite sheet seamlessly wrapped into a cylindrical tube. MWNTs are composed of coaxial nanotube cylinders, of different helicities, with a typical spacing of ~0.34 nm, which corresponds closely to the inter-layer distance in graphite of 0.335 nm [11]. There are different types of CNTs depending on the orientation of the tube axis relative to the carbon network, which are described by the indices of the chiral vector, n and m. Armchair CNTs ($n = m$) usually show metallic conductivity while zigzag ($m = 0$) or chiral ($n \neq m$) CNTs are semiconducting [12, 13]. SWNTs and MWNTs are usually made by carbon-arc discharge, laser ablation of carbon, or chemical vapor deposition (typically on catalytic particles) [14]. The excellent mechanical and electronic properties of carbon nanotubes result from their quasi-one-dimensional (1D) structure and the graphite-like arrangement of the carbon atoms in the shells. Thus, the nanotubes have high Young's modulus and tensile strength, which makes them preferable for composite materials with improved mechanical properties. The electronic band structure of the nanotube can be described by considering the bonding of the carbon atoms arranged in a hexagonal lattice. Each carbon atom ($Z = 6$) is covalently bonded to three neighbor carbons via sp^2 molecular orbitals. The fourth valence electron, in the p_z orbital, hybridizes with all the other p_z orbitals to form a delocalized π-band [15]. SWNTs can be either metals or semiconductors depending on the chirality (the chiral angle between hexagons and the tube axis), which have relatively large band gaps (~0.5 eV for typical diameter of 1.5 nm) or small (~10 meV) [16]. The electronic properties of perfect MWNTs are rather similar to those of perfect SWNTs, because the coupling between the cylinders is weak in MWNTs. Because of the nearly one-dimensional electronic structure, electronic transport in metallic SWNTs and MWNTs occurs ballistically (i.e., without scattering) over long nanotube lengths, enabling them to carry high currents with essentially no heating [17].

Nanowires are an important class of 1D materials that have been attracting a great deal of interest in recent years. Nanowires are regarded as an alternative to

CNTs because it is easier to control their electrical properties. As long as the surface is properly passivated (something that occurs naturally during or right after growth), they are invariably semiconducting. The 1D semiconductors usually exhibit excellent electronic, optical, mechanical, thermal, and chemical properties, which lead to various applications ranging from chemical, biological, and environmental sensors and field-effect transistors to logic circuits [18]. Silicon nanowires (SiNWs) are one of the most important 1D semiconductors. With doped p type and n type, SiNWs can be assembled to form p-n junctions, bipolar transistors, and complementary inverters. Thus, SiNWs may be the crucial components for nanoscale electronics [19]. SiNWs may be fabricated through both "top-down" (i.e. through lithographic patterning) and "bottom-up" (chemical synthesis of SiNWs) approaches. The methods include chemical vapor deposition, laser ablation, vapor transport and condensation, molecular beam epitaxy, annealing on silicon, solution growth, and catalytic etching [20]. Among them, chemical vapor deposition, vapor transport condensation, and annealing of catalytic nanoclusters on silicon have been commonly used for their simplicity, minimal equipment needs, and large-scale production capability [21]. The properties of nanowires are determined by the surface area to volume ratio and defects. NWs can possess good electronic and optical properties, such as enhanced ohmic contact resistance, carrier depletion, which can severely influence electrical conduction and surface passivation abound [22]. On the other hand, silicon nanowires are rodlike systems constructed around a single-crystalline core. When there are sufficiently small diameters and a strong anisotropy, most of their properties emerge: the band gap, the Young's modulus, the electrical conductance, or the specific heat [23]. A fundamental modification of electronic properties from the bulk can be evidenced in SiNWs. For example, the indirect bandgap (e.g., ~1.1 eV) between the conduction band minimum and the valence band (VB) maximum of bulk Si could be modified to a direct bandgap due to quantum confinement effects of SiNWs. The diameter dependence of the dopant ionization efficiency, the influence of surface traps on the charge carrier density and the charge carrier mobility in silicon nanowires are the three effects essential for the conductivity of a silicon nanowire [24].

Among the different metal nanoparticles, gold nanoparticles (AuNPs) have a rich history in chemistry. Dating back to ancient Roman times, they were used to stain glasses for decorative purposes. The modern era of AuNP synthesis began over 150 years ago, Michael Faraday was possibly the first to observe that colloidal gold solutions have properties that differ from bulk gold [25]. Due to the distinct optical and electronic properties, AuNPs attract particular interest and are widely used [26, 27]. A wide array of solution-based approaches has been developed in the past few decades to control the size, shape, and surface functionality of AuNPs. The top-down method of AuNPs produces nanoparticles by shattering from bulk gold, while the top-up method involves building up of nanomaterials starting from the atomic level. Typically, the top-up preparation of AuNPs by chemical reduction of gold ions from a solution involves two major parts: (1) reduction of a gold precursor to produce the Au (0) and (2) stabilization of the obtained AuNPs by suitable

stabilizing or capping agents which prevent aggregation of nanoparticles from forming metallic precipitate [28]. Bulk gold is known as a shiny, yellow noble metal that does not tarnish, has a face-centered cubic structure, is non-magnetic, melts at 1336 K, and has density a 19,320 g/cm. However, a nanostructure containing the same gold is quite different: 10-nm particles absorb green light and thus appear red. The melting temperature decreases dramatically as the sample size goes down [29]. Moreover, it was revealed that AuNPs show efficient catalytic activity, particularly those below 10 nm in size. As the particle size of gold is smaller than 2 nm, the valence and conduction bands become narrower, and a gap appears between them causing the metallic character to disappear [30]. Nevertheless, the key characteristic that distinguishes AuNPs from many other nanomaterials is their unique optical properties resulting from a physical phenomenon known as localized surface plasmon resonance (LSPR), which is present typically in nanostructures of plasmonic materials, such as gold, silver, copper, and aluminum. LSPR involves coherent oscillation and excitation of conduction band electrons on the surface of plasmonic nanostructures. For AuNPs, the irradiation of light can range in the ultraviolet-visible-near infrared (UV-VIS-NIR) spectral region. The conditions for the occurrence of LSPR are known to be highly sensitive to their geometric parameters (e.g., size, shape, and symmetry), the material composition and distribution, as well as the overall arrangement of NPs [31, 32]. Electrical conductivity of AuNPs decreases with a reduced dimension due to increased surface scattering, and the surrounding conditions are also important [33]. The gold nanoparticles are generally dispersed in or combined with other materials, that the dispersing process and preparation methods are important in nanofabricaton. A number of studies have shown that the electrical and mechanical properties of the conducting polymers can be improved by the incorporation of gold nanoparticles [34].

Silver nanoparticles (AgNPs) are nanoparticles of silver which are in the range of 1 and 100 nm in size. AgNPs are known to exhibit antimicrobial/antiviral properties, superior catalytic activity and improved enhancement factors for surface-enhanced Raman spectroscopy (SERS) [35, 36]. Silver also has the highest electrical and thermal conductivity among all metals, making it an ideal component for electrical interconnection, though AgNPs toxicity has been demonstrated and raised concerns for the safety when intended to use in biomedical products in vivo [37–39]. In AgNPs, the electrons move freely in the conduction band and valence band which lie very close to each other [36]. Because of surface scattering, the effective resistivity of a nanoscale metal film or wire is higher than the bulk value. However, the scatter of the silver nanoparticle is random variations in the resistance of the contacts, thus AgNPs largely retain the electrical conductivity of the bulk material [40]. For example, the silver nanoparticle-filled polymer composites can be used as conductive adhesives, which meet the demand of preparing conductive polymer composites achieving the highest electrical and/or thermal conductivity [41].

2.2.3 *Summarization of Physical Properties for Conductive Scaffolds*

In the following Table 2.1, scaffolds that reported electrical properties and/or mechanical properties in literatures cited in this chapter are collected and summarized for comparisons that may help to gain insights of roles of the conductivity. It is noted from the tables that the conductivity is determined by various kinds of measurement from different laboratories, and the range of the conductivity value for those scaffolds is quite wide, from semiconductive to conductive to some extents, and those scaffolds not reported the conductivity and mechanical properties are not included in Table 2.1.

2.3 Conductive Scaffolds in Myocardial Tissue Regeneration

Cardiovascular diseases are the leading cause of morbidity and mortality in the world, also resulting in huge economic burdens on national economies. Among those, myocardial infarction (MI) is the most frequently identified specific cause of dilated cardiomyopathy, leading to symptomatic congestive heart failure over time. The main reasons are that nonconductive scar tissue formed in the infarct region after myocardial infarction, which interrupts the electrical communication between adjacent cardiomyocytes, resulting in the propagation of electrical impulse and the delay of regional contraction, contributes to ventricular dysfunction that are common in heart after myocardial infarction (MI); at the same time, the regional structural changes, especially in left ventricular (LV) remodeling after MI can lead to global LV geometric change, which contributes to an increase in LV wall stress and mitral regurgitation [42].

A cardiac patch strategy is a promising option to regenerating an infarcted heart. Besides applying biocompatible scaffolds with or without cells acting as the patch, it has been recognized gradually that conductive scaffolds can contribute more to restore impulse propagation to synchronize contraction and restore ventricular function by electrically connecting isolated cardiomyocytes to intact tissue, allowing them to contribute to global heart function. Meanwhile, it should be emphasized that when designing scaffolds for heart tissue regeneration, mechanical stiffness of the scaffolds should be particularly taken considerations as well as the electrical conductivity, because the scaffolds have to withstand the continuous stretching/relaxing motion of the myocardium that occurs during each heartbeat as well as to provide mechanical support to prevents cardiac remodeling and to improve LV function after MI [43]. Therefore, appropriate stiffness and conductivity are both important factors for scaffolds to enhance cardiomyocyte maturation and to support the contractile and physiological loads of heart tissue. In the past years, a considerable amount of effort has been devoted toward the development of biomimetic scaffolds for cardiac tissue engineering. The major challenges include that most of the

Table 2.1 Summary of conductive scaffolds for tissue engineering and regeneration

Electrical active component	Scaffold	Conductivity	Young's modulus (unless noted)	References
Cardiac tissue				
Conductive polymers	PPY grafted to chitosan sidechain, hydrogel	0.005–0.03 S/m	2–6 kPa	[46, 47]
	PPY grafted to chitosan sidechain was integrated to gelfoam GelMA to form 3D patches	~0.012 S/m	Tensile strength: ~20 kPa; ultimate strain: ~120%	[48]
	PPY-GelMA nanoparticles blended in electrospun film of GelMA/PCL by crosslinking	0.025–0.3 S/m		[51]
	PPY deposited on the acid-modified silk fibroin patterned with nanoscale ridges and grooves	Resistivity: 200–500 Ω/sq (corresponding to ~1 S/cm)	Tensile strength: ~7 MPa Elastic modulus: ~200 MPa	[52]
	PANi/poly(glycerol sebacate), casting film	0.129–1.77 S/m	2.4–6.3 MPa	[114]
	PANi-contained gelatin, electrospun fibers	1–2.1 S/m	499–1384 MPa	[54]
	Electrospun PANi blended with PLGA, followed by HCL doping	0.31 S/m	91.7 MPa	[55]
	PANi blended with PLA, electrospun fibers	2.1×10^{-5} S/m		[56]
	PANi coating on chitosan films micropatterned with a re-entrant honeycomb (bow-tie) pattern	1-direction: 9.3 S/m 2-direction: 2.4 S/m	6.73 MPa	[57]
	Poly (thiophene-3-acetic acid) and methacrylated aminated gelatin (MAAG)	0.01 S/m	22.7–493.1 kPa	[60]
	PLA mixed with PANi as core, PLA and PEG composed the out layer, electrospun fibers	$0.23–0.99 \times 10^{-4}$ S/m	39 MPa	[58]
	PANi on tissue-culture-treated polystyrene, drop-drying	2 kΩ/sq		[53]

Carbon nanomaterials	Graphene	4170 $cm^2/V\ s$		[72]
	Graphene patterned with ridges	7.0 kΩ		[73]
	rGO blended with GelMA	1.5–4 kΩ	22.6 kPa	[79]
	Graphene/collagen biohybrid, casting	0.65 S/m	0.77–1.29 MPa	[74]
	Collagen scaffolds coated covalently with GO reduced in 2% sodium hydrosulfite	3.8–29 × 10^{-4} S/m	160–750 kPa	[75]
	rGO/methacryloyl-substituted tropoelastin	~1 kΩ under 10 Hz	19.3 kPa	[77]
	Graphene blended with PCL, electrospun fibers	1.5 × 10^{-11} to 1.5 × 10^{-8} S/m		[78]
	rGO blended with silk fibroin, electrospun fibers	4.3 kΩ	~12.5 MPa	[76]
	GO with oligo(poly(ethylene glycol) fumarate, injectable hydrogel	0.42 S/m		[80]
	GO incorporated in PEGDA700-Melamine crosslinked with thiol-modified hyaluronic acid	0.03 S/m	25 Pa	[81]
	Gold nanoparticle-modified GO blended with chitosan	0.012 S/m		[93]
	MWCNTs blended with GelMA	~2.2 kΩ under 1 Hz	20–54 kPa	[70]
	SWCNTs blended with poly (*N*-isopropylacrylamide), hydrogel	1.08 × 10^{-4} Ω^{-1}		[71]
	SWCNTs blended with collagen, hydrogel	1.72 × 10^{-6} S/m		[96]
	SWNTs/gelatin, hydrogel	5 × 10^{-5} S/m		[61]
	CNT dispersed in aligned poly(glycerol sebacate): gelatin, electrospun nanofibers	~5 kΩ under 100 Hz	Tensile strength: ~1.4 MPa	[65]
	Injectable reverse thermal gel functionalized with MWCNTs	6.93 × 10^{-4} S/m	Shear modulus: 221 Pa	[63]
	CNTs blended with 124 polymer	60.9–76.2 kΩ	1.6–2.2 MPa	[64]
	CNTs blended with polycaprolactone and silk fibroin, aligned nanofiber yarns	6.5–8.1 × 10^{-5} S/m	In sutures warp direction: 110 MPa; in weft direction: 20 MPa	[68]
	MWCNT sprayed on polyurethane electrospun film	0.005–2.13 S/m	2.32–5.83 MPa	[66]
	Carbon fibers blended with PVA, hydrogel	0.3 S/m	2.3 MPa	[99]

(continued)

Table 2.1 (continued)

Electrical active component	Scaffold	Conductivity	Young's modulus (unless noted)	References
Gold nanoparticles (GNPs)	GNPs blended with chitosan, hydrogel	0.13 S/m	6.8 kPa	[86]
	GNR blended with GelMA, bioprinting	12.0 kΩ under 20 Hz 5.0 kΩ under 100 Hz	4.7 kPa	[90]
	GNRs/GelMA, hydrogel	810 Ω under 20 Hz 700 Ω under 100 Hz	1.3 kPa	[89]
	GNPs blended with HEMA	15.3 S/m	0.6–1.6 MPa	[85]
	GNPs blended with reverse thermal gel	140.1 kΩ	0.26 kPa	[88]
	GNPs deposited on fibrous decellularized matrix	~285 Ω		[92]
	Gold nanorods (GNRs)/GelMA Silica nanoparticles (SNP) blended with GelMA	GNRs/GelMA: 2.5 kΩ under 20 Hz SNP/GelMA: 30.77 kΩ under 20 Hz	GNR/GelMA: 1.37 kPa SNP/GelMA: 0.55 kPa	[98]
Nerve				
Conductive polymers	PPY blended with PDLLA	5.65–15.56 mS/cm		[124]
	PPY blended with polyphenol/tannic acid, hydrogel	0.05–0.18 S/cm	0.3–2.2 kPa	[126]
	PPY/hyaluronic acid with CNTs	12.59 kΩ under 1 Hz 1.67 kΩ under 10 Hz	3.17 kPa	[136]
	PANi in poly (epsilon-caprolactone)/gelatin, electrospun nanofibers	2.4×10^{-8} Ω^{-1}	Tensile strength: 8.19–8.75 MPa	[122]
	PANi blended with polyethylene glycol diacrylate	1.1×10^{-3} mS/cm		[123]
	poly(glycerol sebacate) mixed with aniline pentamer conjugated with polyurethane	1.4×10^{-6} to 8.5×10^{-5} S/cm	5.6–75.5 MPa	[127]

Carbon nanomaterials	Graphene on tissue culture plate	350 Ω (50 μm × 50 μm)		[128]
	rGO blended with poly(3,4-ethylenedioxythiophene)	0.017–0.025 S/m	84 MPa	[132]
	Single layered graphene (SG) or multilayered graphene (MG) coated with PDA/RGD and polycaprolactone (PCL), 3D printing and layer by layer casting	SG/PCL: 0.89 S/m MG/PCL: 0.64 S/m	SG/PCL: 68.74 MPa MG/PCL: 58.63 MPa	[130]
	highly-conductive few-walled-CNT (fwCNT) blended with gum Arabic	3000 S/cm		[137]
	agarose modified carbon nanofibers, wet spinning	145 S/cm	LN+: 867 MPa	[133]
	CNT/chitin, plasma-treated	2.89 S/m	420 MPa	[135]
	SWCNTs modified by PPY and blended with hyaluronic acid	12.59 kΩ under 1 Hz 1.67 kΩ under 10 Hz	3.17 kPa	[136]
Skeletal				
Conductive polymers	PANi blended with PCL, electrospun fibers,	63.6 mS/cm	55.2 MPa	[117]
	Grafting aniline pentamer to poly(ethylene glycol)-co-poly(glycerol sebacate)	1.84×10^{-4} S/cm	24.6 MPa	[115]
	Self-healable conductive injectable hydrogels synthesized by tetramer-graft-4-formylbenzoic acid /*N*-carboxyethyl chitosan	$2.7–3.4 \times 10^{-2}$ mS/cm	The storage modulus: 300–600 Pa	[116]
Carbon nanomaterials	r(GO/PAAm), Casting film	$1.3–1.4 \times 10^{-4}$ S/cm	r(GO/PAAm): 49–57 kPa	[113]
	GO/PCL, electrospun fibers	10^{-7} S/m	Tensile strength: 4.0 MPa	[108]
	GO and hydroxyapatite nanoparticles, hydrogel	0.12–0.2 S/m	200–320 kPa	[110]
	MWCNT/PLA, electrospun fibers	Random: 1×10^4 Ω/sq Aligned: 1×10^3 Ω/sq	Random: 20–80 MPa Aligned: 40–90 MPa	[107]
	MWCNTs membrane functionalized by the [4 + 2] Diels–Alder cycloaddition reaction of 1,3 butadiene	3×10^3 S/m		[105]

(continued)

Table 2.1 (continued)

Electrical active component	Scaffold	Conductivity	Young's modulus (unless noted)	References
Wound				
Conductive polymers	Quaternized chitosan grafted with polyaniline blended with benzaldehyde group functionalized poly(ethylene glycol)-co-poly(glycerol sebacate), hydrogel	2.25–3.5 mS/cm	58–368 Pa	[138]
	Oxidized hyaluronic acid-graft-aniline tetramer/*N*-carboxyethyl chitosan, hydrogel	0.1–0.45 mS/cm	Shear modulus: 0.13–1.40 kPa	[139]
Carbon nanomaterials	rGO/hyaluronic acid graft dopamine	$(1.2–2.5) \times 10^{-4}$ S/m	Shear modulus: 0.32–0.42 kPa	[147]
	Polydopamine-reduced GO dispersed in mixture of chitosan and silk fibroin, freeze-drying	0.05–0.25 S/cm	Compressive strength: 60–90 kPa	[146]
	CNTs blended with glycidyl methacrylate functionalized quaternized chitosan	0.04–0.12 S/m		[148]

polymers to be used as scaffolds are electrically insulating, and scaffolds lack the structural and mechanical robustness to engineer cardiac tissue constructs with suitable electrophysiological functions. Strategies to overcome the problems are incorporating conductive polymers or/and conductive nanomaterials into polymeric materials to bring the electrical conductivity to the scaffolds, and the incorporated conductive materials can increase the stiffness of the scaffolds at the same time. In addition, the conductive engineered cardiac tissue-like constructs are also expected to provide a powerful platform for drug screening and assessment of cardiac toxicity in vitro, because they are simple, fast, relatively cheap, and require fewer animals, therefore would be a significant advancement for developing new drugs and have led to a growing interest in recent years.

2.3.1 Composite Scaffolds Containing Conductive Polymers

2.3.1.1 Polypyrrole

Polypyrrole (PPY) is a well-known conductive polymer in tissue engineering. However, as introduced before, PPY is a non-thermal plastic, mechanically rigid, and brittle. Hence, it is usually conjugated to or just blended with insulating polymers for fabricating conductive scaffolds. By this way, its biocompatibility is improved due to compositing with other polymers and the resulting scaffolds obtained improved conductivity [44, 45].

Hydrogels containing PPY have been widely investigated. Chitosan is biodegradable, produces minimal immune reaction in humans, and has been used extensively as a biomaterial for decades. For example, when PPY was grafted to chitosan side chain by a chemical oxidative polymerization, a PPY-chitosan hydrogel could be generated, which did not reduce the attachment, metabolism, or proliferation of rat smooth muscle cells (SMCs) in vitro. Importantly, the PPY-chitosan hydrogels formed hysteresis loops when subjected to a cyclic voltammetry, suggesting they are semiconductive, whereas ungrafted chitosan was not. When neonatal rat cardiomyocytes were seeded on the semiconductive hydrogel, they showed enhanced Ca^{2+} signal conduction in comparison with those on the chitosan alone. In addition to the semiconductivity, the PPY-chitosan had good mechanical properties and was injectable, these features collectively in turn significantly improved border zone conduction velocity with improved cardiac function around the scar of rat hearts after MI [46]. Furthermore, the PPY-chitosan injected was reported to form a hydrogel in situ and restore tissue conductivity of the scar and re-establish synchronous ventricular contraction, which were evidenced by the improvement of electrical impulse propagation across the scarred tissue and the decreased QRS interval, whereas saline control or chitosan alone continued to have delayed propagation patterns and significantly reduced conduction velocity compared to healthy controls [47]. When the PPY-chitosan was integrated with a conventional gelfoam GelMA (methyl acrylic anhydride-gelatin), the two components formed a three-dimensional conductive

patch (PPY-chitosan+GelMA) used to support cardiomyocyte (CM) viability and function in vitro. The PPY-chitosan+GelMA patch not only showed a higher mean breaking stress but also showed higher conductivity than GelMA or GelMA soaked with chitosan (chitosan+GelMA) in the ex vivo conductivity testing. As a result, the Ca^{2+} transient velocity of cardiomyocytes cultured on the conductive patch was 2.5-fold higher than that of cardiomyocytes cultured on GelMA or chitosan+GelMA. When the patches were implanted in a full-thickness right ventricular outflow tract defect of rats, the patch-implanted hearts had faster conduction velocities, as measured on the epicardial surface by optical mapping at 4 weeks post-implantation. Furthermore, the composite looked biocompatible, since continuous electrocardiographic telemetry did not reveal any pathologic arrhythmias after patch implantation and noted that there was higher inflammatory cell infiltration in the two control groups compared with the conductive GelMA patch [48].

Besides combined with hydrogels, PPY can be integrated into nanofibrous scaffolds by utilizing electrospinning technique. It is well documented that nanofibrous structures are to some extent like that of natural extracellular matrix, and electroactive scaffolds that provide topographical cues as well as electrical and mechanical properties are attractive and have been largely investigated in the past decades. One of the simple approaches of generating conductive nanofibers was to have poly(lactic-co-glycolic acid) (PLGA) fibers coated with PPY, the resulting product was named as electromechanically active fiber scaffold. Interestingly, the scaffold was reported to be capable of generating mechanical actuation through the volume change of the individual fibers as well as delivering direct electrical stimulation to induced human pluripotent stem cells (iPS). By this way, the scaffold increased the expression of cardiomyocyte-specific genes (*Actinin*, *NKX2.5*, *GATA4*, *Myh6*, *c-kit*) and downregulated the expression of stemness genes (*Oct4*, *Nanog*) for both electrical stimulated and unstimulated protocols, and the scaffold while exhibiting no cytotoxic effects on the iPS [49]. Nevertheless, the biocompatibility of high concentrations of PPY remains controversial, higher than 9.7 μg/mL PPY polymerized by oxidative doping has been considered harmful for cell viability/proliferation [50]. To overcome this challenge, a research group proposed an approach to reduce the amount of PPY but to retain the necessary conductivity: to integrate conductive nanoparticles composed of GelMA and PPY with electrospun nanofibrous membrane composed of polycaprolactone (PCL) and GelMA (ES-GelMA/PCL) following the separate preparations. First step was to prepare the conductive nanoparticles (GelMA-PPY); next, the GelMA-PPY nanoparticles were uniformly crosslinked on the ES-GelMA/PCL membrane, the more deposition of conductive nanoparticles, the higher conductivity the scaffold had. In addition, GelMA-PPY nanoparticles brought rough topography to the nanofibrous membrane, which was considered beneficial to the vascularization in vitro. The conductive scaffolds enhanced the function of cardiomyocytes and yielded their synchronous contraction. After implanted on the infarcted heart for 4 weeks, the conductive membrane had the infarct area decreased by about 50%, the left ventricular shortening fraction percent was increased by about 20%, and the neovascular density in the infarct area was significantly increased by about nine times compared with that in the MI group [51].

PPY was also used in nanostructural patterns that are extracellular cues to guide cell proliferation and differentiation. For example, through polymerization on surface, PPY was deposited directly on the acid-modified silk fibroin-patterned nanoscale ridges and grooves mimicking of native myocardial extracellular matrix (ECM) topography, which made a remarkable reduction of resistance for the silk fibroin film, from 10^6 Ω/sq for the unmodified sheet to the range of 200–500 Ω/sq [52]. Consequently, the patterned conductive substrates maintained high cell viability over 21 days incubation, meanwhile, the structural and functional properties of cultured human pluripotent stem cells (hPSC)-derived cardiomyocytes were enhanced due to the electroconductive and the anisotropic topographical cues, evidenced by the increase of cellular organization and sarcomere development and significantly upregulated the expression and polarization of connexin 43 (Cx43) and the expression of genes that encode key proteins involved in regulating the contractile and electrophysiological function of mature human cardiac tissue.

2.3.1.2 Polyaniline and Derivatives

Another frequently investigated conductive polymer is polyaniline (PANi) that is a substance polymerized chemically or electrochemically with monomeric aniline. In an earlier literature, a group investigated the adhesion and proliferation properties of rat cardiac myoblast H9c2 cells on the polyaniline substrate. It was reported that the conductive polyaniline allowed for cell attachment and proliferation. In comparison with tissue-culture-treated polystyrene (TCP), the initial adhesion of H9c2 cells to the conductive PANi was slightly reduced by 7%, but the overall rate of cell proliferation on the conductive surfaces was like that on the control TCP surfaces. After 6 days in culture, the cells formed confluent monolayers which were morphologically indistinguishable. However, the stability of conductivity remained a challenge. Although the conductive PANi retained a significant level of electrical conductivity for at least 100 h in an aqueous physiologic environment, the conductivity gradually decreased by about three orders of magnitude over time [53]. It is easy to fabricate conductive scaffolds by blending PANi with various kinds of polymers. For example, PANi was able to be blended with gelatin and co-electrospun into nanofibers. The blend fibers containing less than 3% PANi in total weight showed uniform morphology without phase segregation, and interestingly, the average diameter of fibers was reduced from 803 nm to less than 100 nm, and the tensile modulus increased from 499 to 1384 MPa, due to the addition of PANi. The resulting fibrous scaffolds could support rat cardiac myoblast H9c2 cell attachment and proliferation, and the cells grown on the fibers of smaller diameter showed more stressful morphology [54]. A mesh made of aligned nanofibers of PANi and poly(lactic-co-glycolic acid) (PLGA) was reported to be able to attract negatively charged fibronectin and laminin that are beneficial to enhance cell adhesion. The adhered cardiomyocytes became connected to each other and formed isolated cell clusters; the cells within each cluster elongated and aligned their morphology along the major axis of the fibrous mesh, and the cardiomyocytes within each cluster beat

synchronously. At the same time, the gap-junction protein connexin 43 was observed upregulated, implying that the cells have developed coupling between each other. Furthermore, the beating rates among these isolated cell clusters were capable of being synchronized under an electrical stimulation imitating that generated in a native heart, which is an important feature, because the impaired heart function depends on electrical coupling between the engrafted cells and the host myocardium to ensure their synchronized beating [55]. Similar conductive nanofibrous sheets composed of poly(L-lactic acid) (PLA) blending with PANi were reported for cardiac tissue engineering and cardiomyocyte-based 3D bioactuators. By incorporating PANi up to 3 wt% into the PLA polymer, the electrospun nanofibrous sheets gained enhanced conductivity. These conductive nanofibrous sheets not only enhanced the cell–cell interaction, maturation, and spontaneous beating of primary cardiomyocytes but were also a kind of suitable fundamental material to fabricate cardiomyocyte-based 3D bioacutuators. The folding bioactuator formed by cardiomyocyte-laden PLA/PANi displayed stronger spontaneous contraction at 1.6 Hz and displacement without any trigger, which was driven by synchronous beating of the cardiomyocytes than that formed by cardiomyocyte-laden PLA nanofibrous sheets [56]. The blend of chitosan and PANi was employed to process a re-entrant honeycomb pattern that can provide negative Poisson's ratio, aiming to obtain the auxetic behavior for scaffolds of cardiomyocytes. It is known that the Young's modulus of native human heart varies from 0.02 to 0.50 MPa depending on whether the heart is in systole or diastole, with infarct tissue being even stiffer. In order to meet the demand of cardiomyocytes contracting on scaffolds, auxetic behavior can be imparted into a material. The scaffold design addressed the match of dynamic mechanical properties between heart tissue and cardiac patch. The micropattern of the re-entrant honeycomb structure was developed by using excimer laser microablation, which produced patches that could be tuned to match native heart tissue. The resulting scaffolds with the ultimate tensile strength and strain at failure of 0.06–1.53 MPa and 27–96%, respectively, are comparable to the reported values for native human heart tissue. The patches were determined to have Poisson's ratios in the range of −1.45 to −0.15. It is noticeable that the conductivity of the patterned patches was also anisotropic and maintained a similar level of conductivity compared to the unpatterned patches composed of the same composite. As an encouraging result, the auxetic patches were cytocompatible with murine neonatal cardiomyocytes in vitro and had no detrimental effect on the electrophysiology of both healthy and MI rat hearts and conformed better to native heart movements than unpatterned patches of the same material in ex vivo. Besides, the implantation in a rat MI model for 2 weeks had not shown detrimental effects on cardiac function, and negligible fibrotic responses were detected [57].

Like PPY, the biocompatibility of PANi is still a concerned issue. To avoid the potential toxicity of PANi to cardiomyocytes grown on the nanofibrous scaffold, a group fabricated a kind of core–shell fiber using coaxial electrospinning technique. The mixture of poly(lactic acid) (PLA) and PANi doped with dodecylbenzenesulfonic acid (DBSA) was used as the component of the core, and the mixture of PLA and poly(ethylene glycol) (PEG) was taken as the out layer of the fiber. Interestingly,

the incorporation of PEG could enhance the packing of PLA and PANi chains. The PANi and PEG affected the thermal and electrical properties of the fibers, both decreasing the glass transition temperature and increasing the electrical conductivity, and at the same time, the biocompatibility of the core-shell fibers increased [58]. Another strategy of avoiding the potential cytotoxicity of PANi was to have PANi grafted to the backbone of chitosan molecules. For example, PANi was grafted to the backbone of quaternized chitosan. The resulting hydrogel gained the conductivity similar to that of native cardiac tissue (~10^{-3} S/cm) and showed good biocompatibility with adipose-derived mesenchymal stem cells (ADMSCs) as well as the H9C2 cardiac cells and myoblasts C2C12 cells [59]. Besides PPY and PANi, some new conductive polymers have been explored for uses in the fabrication of conductive scaffolds. For example, a homogeneous electronically conductive double network hydrogel (HEDN) was fabricated by a rigid, hydrophobic and conductive network of chemical crosslinked poly(thiophene-3-acetic acid) and a flexible hydrophilic biocompatible network of photo-crosslinking methacrylated aminated gelatin. By adjusting the component ratio, the swelling, mechanical, and conductive properties of HEDN hydrogel could be modulated. The Young's moduli for the resulting double network hydrogel varied from 22.7 to 493.1 kPa, and its conductivity was about 0.01 S/m, falling in the range of the conductivity for native myocardium tissue. The hydrogel is biocompatible, could well support brown adipose-derived stem cells survival and proliferation, as well as improve the cardiac differentiation of the stem cells and electrical stimulation can further improve this effect [60].

2.3.2 Conductive Scaffolds Containing Inorganic and Metal Nanoparticles

It has been widely recognized that conductive nanoparticles are ideal contents to bring conductivity and nano-scale topography to scaffolds, as well as to reinforce mechanical properties of the scaffolds. Carbon nanotubes, grapheme, gold nanoparticles, silicon wire, and silver nanoparticles are mostly investigated ones.

2.3.2.1 Carbon Nanotubes

Carbon nanotubes (CNTs) can be easily incorporated with various kinds of hydrogels. For example, SWNTs were incorporated into gelatin hydrogels to construct three-dimensional engineered cardiac tissues. The SWNTs in the hydrogel could provide cellular microenvironment in vitro favorable for cardiac contraction and increased the expression of electrochemical associated proteins Cx43 and TnT. Upon implantation into the infarct hearts in rats, the engineered cardiac tissues structurally integrated with the host myocardium, with different types of cells observed to

mutually invade into implants and host tissues, showing essential roles of SWNTs to improve the performance of ECTs in inhibiting pathological deterioration of myocardium [61]. In another research, by blending single-walled carbon nanotubes at subtoxic concentrations with a gelatin-chitosan hydrogel, a composite hydrogel was developed, in which the SWCNTs were designed to act as electrical nanobridges between cardiomyocytes, resulting in the enhancement of electrical coupling, synchronous beating, and cardiomyocyte function. The conduction velocity of NRVM cultured in hydrogels containing SWNTs was ~23 cm/s, which was significantly faster than NRVM cultured in hydrogels without SWNTs, and close to ~27 cm/s in 10-day-old neonatal rat heart [62]. When conjugated with an injectable reverse thermal gel (RTG), multiwalled carbon nanotubes (MWCNTs) brought conductivity to RTG, which transited from a solution at room temperature to a three-dimensional (3D) gel-based matrix shortly after reaching body temperature (RTG-CNT). The resistance of MWCNTs functionalized with –COOH was 24.3 kΩ, and RTG-CNT had a resistance of 144.3 kΩ at 37 °C. The 3D RTG-CNT system supported long-term CM survival, promoted CM alignment and proliferation, and improved CM function when compared with traditional two-dimensional gelatin controls and 3D RTG system without CNTs [63].

Casting is a facile approach to introduce carbon nanotubes (CNTs) into synthetic polymers. An elastomeric film was produced by blending multiwalled carbon nanotubes (MWCNTs) into poly(octamethylene maleate (anhydride) 1,2,4-butanetricarboxylate) (124 polymer) for cardiac tissue engineering, in which the MWCNTs provided electrical conductivity and structural integrity to 124 polymer. The 124 polymer with 0.5% and 0.1 wt% MWCNTs exhibited improved conductivity and swelling against pristine 124 polymer. The bulk modulus of composite film was increased proportionally to the MWCNT content while the bulk modulus was decreased. Consequently, the excitation threshold of engineered cardiac tissue on the film with 0.5% MWCNTs was 3.6 V/cm, significantly shorter than 5.1 V/cm of the control and 5.0 V/cm of 0.1% CNTs, suggesting greater tissue maturity due to the electrical and mechanical advantages of the scaffolds [64]. Besides integrating in casting films, multiwalled carbon nanotubes can also be dispersed in aligned poly(glycerol sebacate):gelatin (PG) electrospun nanofibers (CNT-PG) to enhance the fibers' alignment and improved the electrical conductivity and toughness of the scaffolds. The CNT-PG was observed to maintain the viability, retention, alignment, and contractile activities of cardiomyocytes, leading to a stronger spontaneous and synchronous beating behavior, the cells showing 3.5-fold lower excitation threshold and 2.8-fold higher maximum capture rate compared to those cultured on the nonconductive PG scaffold after 7-day culture, no matter with or without electrical stimulations [65]. Multiwalled carbon nanotubes (MWCNTs) could be combined with polyurethane nanofibers by electrospray technique to generate electroconductive nanofibrous patches. The MWCNTs were reported to well adhere on the polyurethane nanofibers that created an interconnected web-like structures, and the MWCNT content could reach to 0.2 wt%, 0.3 wt%, and 0.6 wt% when deposited in the nanofibrous patches. The addition of MWCNTs decreased the diameter of the nanofibers and significantly enhanced the electrical conductivity, tensile strength,

Young's modulus, and hydrophilicity of the nanocomposites. Importantly, the scaffolds showed better cytocompatibility and improved interactions between the scaffold and cardiomyoblasts. Noted that the composite nanofibrous patches also friendly enhanced the interactions between scaffolds and endothelial cells, and this would be beneficial to the angiogenesis in the engineered constructs of heart [66]. Similarly, the positive interactions of MWCNT-containing nanofibrous polyurethane to human umbilical vein vascular endothelial cells were reported by our previous work. The aligned nanofibrous structure and incorporated MWCNT acted in a coordinated way to promote the endothelial cells to produce type IV collagen, meanwhile the cells seeded on the aligned nanofibrous composite films released significantly lower amounts of tissue factor and PAI-1 than those growing on the control. These results again showed that MWCNTs component embedded in the nanofibrous polyurethane films benefited to the endothelial cells to preserve their anticoagulant functions [67].

An interesting design of scaffold fabricated with aligned conductive nanofiber yarn network was proposed and fabricated with polycaprolactone, silk fibroin, and carbon nanotubes (NFYs-NET). The nanofiber yarn network was intended to mimic the native cardiac tissue structure to control cellular orientation and enhance cardiomyocyte (CM) maturation. When encapsulated within a hydrogel shell, the NFYs-NET layers formed 3D hybrid scaffolds, and these 3D scaffolds promoted aligned and elongated CM maturation on each layer and individually control cellular orientation on different layers in a 3D environment. When CMs were cultured on the NFYs-NET layer, and endothelial cells were within the hydrogel shell, endothelialized myocardium was constructed, as the NFYs-NET layer induced cellular orientation, maturation, and anisotropy, and the hydrogel shell provided a suitable 3D environment for endothelialization [68]. Besides employed as fillers in composites, carbon nanotubes can be used as scaffolds directly to cardiac cells in the form of nonwoven film or mesh. For example, superaligned carbon nanotube sheets (SA-CNTs) were employed to culture cardiomyocytes, mimicking the aligned structure and electrical impulse transmission behavior of the natural myocardium. The SA-CNTs not only induced an elongated and aligned cell morphology of cultured cardiomyocytes but also provided efficient extracellular signal transmission pathways required for regular and synchronous cell contractions. Furthermore, the SA-CNTs reduced the beat-to-beat and cell-to-cell dispersion in repolarization of cultured cells, which is essential for a normal beating rhythm, and potentially reduced the occurrence of arrhythmias. The SA-CNT-based flexible one-piece electrodes also demonstrated a multipoint pacing function. These features make SA-CNTs promising in applications in cardiac resynchronization therapy by enhancing cells to communicate electronic signals [69].

In addition to the conductivity, the function of ROS clearance for carbon nanotubes may contribute to the scaffold-induced tissue regeneration, since ROS would severely impair the adhesion of engrafted stem cells. In one study, carbon nanotubes (CNTs) were incorporated in the gelfoam (GelMA). By seeding neonatal rat cardiomyocytes on the hydrogels, cardiac constructs were developed. Researchers noticed that the addition of CNTs brought an important function to the cardiac patches, that

is, to resist the damage induced by a model cardiac inhibitor heptanol as well as a cytotoxic compound doxorubicin. In this investigation, heptanol or doxorubicin was applied to the cardiac patches for 5-day culture. Heptanol is a widely used reversible inhibitor of cell-to-cell coupling, which prevents gap-junctional permeability of Ca^{2+} and interrupts beating propagation. A rapid disappearance of synchronous beating was observed on the pristine GelMA surface within 20 min, while beating persisted on CNT-GelMA. More CNT addition led to more gradual disturbance to beating rhythm. It means that cardiomyocytes on CNT-GelMA continued to beat synchronously even after the gap junctional beating propagation was inhibited, indicating that the conductive CNT network played a role in propagating calcium transient and action potential between cells. The generation of free oxygen radicals is believed to be the main mechanism for the cardiotoxicity of doxorubicin. When 300 μM of doxorubicin was perfumed into the growth chamber, tissues on pristine GelMAs showed an immediate decrease (>50%) in the beating amplitude, as well as the beating rates, while the amplitude and beat-to-beat variation of cardiac tissues on CNT-GelMA were not significantly affected, which suggests a protective role of CNT against oxidative stress by acting as free radical scavengers, and might be an important feature of carbon nanomaterial-containing scaffolds [70]. Similarly, another research group reported that single-walled carbon nanotubes (SWCNTs) were able to clear ROS after MI. In this study, poly (*N*-isopropylacrylamide) (PNIPAAm) hydrogel was used for encapsulating brown adipose-derived stem cells, and a small amount of SWCNTs were introduced into the hydrogel. Although the conductivity of the resulting hydrogels was only 10^{-4} Ω^{-1}, it could be noticed that in the presence of H_2O_2, the stem cells in the SWCNT-containing hydrogel showed significantly higher bioactivities including promoted cell adhesion and proliferation compared with those in the control hydrogel. Furthermore, the SWCNT-containing hydrogel encapsulating the stem cells could be injected in situ in rats with myocardial infarction and significantly enhanced the engraftment of seeding cells in infarct myocardium and augmented their therapeutic efficacies [71].

2.3.2.2 Graphene and Derivatives

Graphene and graphene derivatives including graphene oxide (GO) and partly reduced GO (rGO) have been extensively employed as novel components to fabricate electrically conductive composites that can effectively deliver electrical signals to biological systems. Graphene is a superconductive material that can be used directly for the growth and differentiation of stem cells and human induced pluripotent stem cells (hiPSCs). The ability of iPS to differentiate into cardiomyocytes provides abundant sources for disease modeling, drug screening, and regenerative medicine; however, hiPSC-derived cardiomyocytes (hiPSC-CMs) display a low degree of maturation and fetal-like properties. To overcome this problem, one example is to seed hiPSCs on graphene sheets. It was assumed that the graphene substrate could facilitate the intrinsic electrical propagation, mimicking the microenvironment of the native heart to promote the global maturation of hiPSC-CMs.

It was reported that the graphene substrate markedly increased the myofibril ultrastructural organization, elevated the conduction velocity, and enhanced both Ca^{2+} handling and electrophysiological properties of the stem cells even without electrical stimulation. On the graphene substrate, the level of connexin 43 increased as well along with the conduction velocity, and the bone morphogenetic protein signaling was significantly activated during the early period of cardiogenesis in RNA level [72]. In some studies, micro- and nano-scale topographies were brought into graphene membranes by specifically processing technology, which have been demonstrated mimicking the extracellular matrix structures to some extent. One group selected polyethylene glycol (PEG) as substrates on which there were ridges and grooves of 800 nm in widths fabricated by using capillary force lithographic techniques. The graphene membrane was placed on the patterned PEG following the oxygen-plasma treatment, which allows them to have more profound effect on cellular phenotype than the pristine graphene membrane. As shown that the tissue constructs displayed the enhancement of myofibrils and sarcomeres and exhibited the expression of cell–cell coupling, meanwhile, calcium-handling proteins were all significantly increased, suggesting that directional electrical conductivity could impact the functional phenotype of cultured cardiac cells [73].

Like carbon nanotubes, graphene can be easily incorporated with various kinds of polymeric materials that are further processed into scaffolds with different nanostructures or blended in hydrogels. By this way, one can design and fabricate conductive scaffolds with controllable mechanical properties and versatile microstructures. For example, collagen and pristine graphene were mixed to prepare a kind of biological composite to harness both the biofunctionality of the protein component and the increased stiffness and enhanced electrical conductivity to matching that of native cardiac tissue. The biological composite containing 32 wt% graphene significantly increased metabolic activity and cross-striated sarcomeric structures of embryonic stem-cell-derived cardiomyocytes, and electrical stimulation further enhanced the alignment and maturation of the embryonic stem-cell-derived cardiomyocytes. In addition, the biological composite also enhanced human cardiac fibroblast growth and simultaneously inhibited the attachment of bacterial such as *Staphylococcus aureus* [74]. Partly reduced graphene oxide (rGO) is also a candidate in the fabrication of conductive composites. Although the oxidation treatment decreases the conductivity of pristine graphene, following partly reduction can restore part of the conductivity of graphene oxide; hence, rGO usually has a higher conductivity than GO while holding better hydrophilic property than pristine graphene. For example, a composite of collagen and graphene oxide (Col-GO) with a reduction treatment was fabricated for uses as a cardiac patch. In the fabrication process, collagen scaffolds were generated using a freeze-drying method, followed by conjugated covalently with GO. At the final step, the scaffold Col-GO was subjected to a reduction treatment by an immersion in 2% sodium hydrosulfite for 3 min. By this way, the electrical conductivity of the final scaffolds fell in the range of semiconductive materials about 10^{-4} S/m. At the same time, the highest tensile strength of the scaffolds could reach to 162 kPa and the Young's modulus to 750 kPa. As for the morphology of the scaffolds, there were randomly oriented

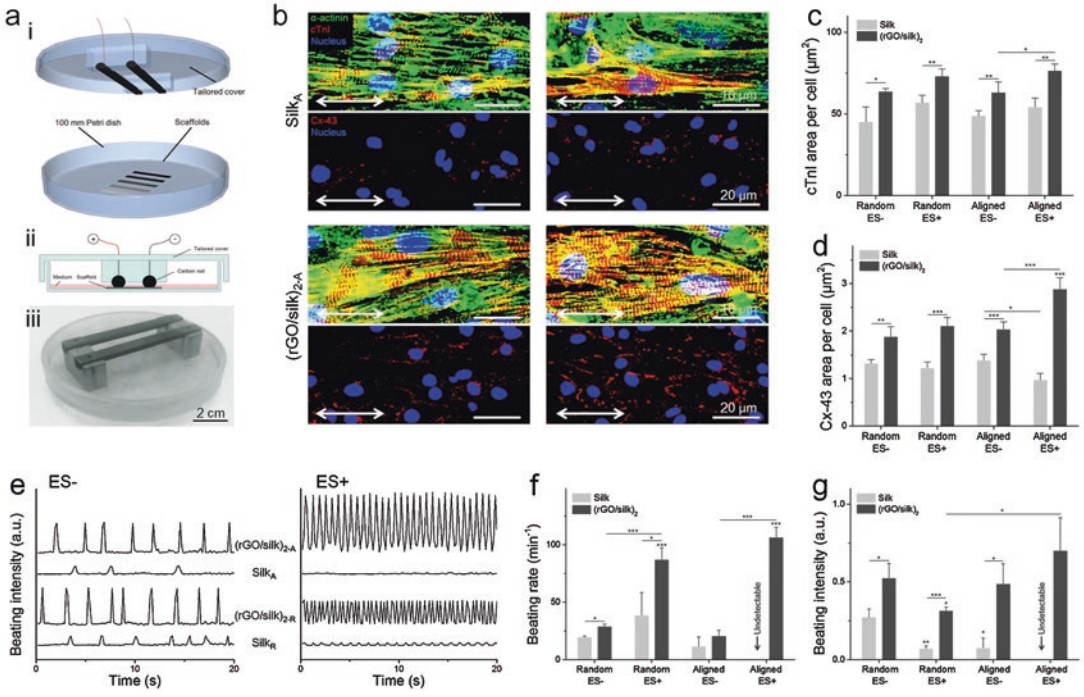

Fig. 2.2 The synergy of electrical stimulation and rGO/silk scaffolds on the functionalities of cardiac tissues. (**a**) (*i*) 3D, (*ii*) 2D schematics, and (*iii*) photograph of a custom-made Petri dish cover (100 mm) that provides parallel electric fields to cells when connected to an electrostimulator. (**b**) Immunofluorescence images showing the expression of α-actinin, cTnI, and Cx-43 for cardiomyocytes cultured on silk and $(rGO/silk)_{2\text{-}A}$ without and with electrical stimulation. The double arrows indicate the orientation of the nanofibers in the aligned groups. (**c**, **d**) Quantitative analysis of (**c**) cTnI and (**d**) Cx-43 expression showing the significantly enhanced formation of calcium ion-sensing sarcomeres and gap junctions in the aligned rGO/silk group with electrical stimulation. (**e**) Beating profiles of cardiomyocytes cultured on silk and $(rGO/silk)_2$ scaffolds without and with electrical stimulation. (**f**, **g**) Statistical analysis of (**f**) the beating rate and (**g**) beating intensity of cardiomyocytes cultured on silk and $(rGO/silk)_2$ scaffolds without and with electrical stimulation [76]

interconnected pores of 120–138 μm in diameter in the Col-GO scaffolds where GO flakes being well distributed in the pore walls. It is interesting and should be noted that the scaffolds showed the function of enhancing angiogenesis as higher VEGF expression observed in the scaffolds collected at 4 weeks after subcutaneous implantation as well as supported neonatal cardiomyocyte adhesion and upregulated the expression of the cardiac genes, including Cx43, Actin4, and Trpt-2 than their non-conductive counterparts [75]. Reduced graphene oxide was also used to modify silk nanofibrous biomaterials with controllable surface deposition on the nanoscale. A reduced graphene oxide (rGO) nanolayer could be attained, and the thickness was well controlled on the silk nanofibrous scaffolds by using a vacuum filtration system. The electrical resistance of the composites was 4.3 kΩ, and the Young's modulus was not affected by the rGO deposition. The composite nanofibrous scaffolds promoted the expression of cardiac-specific proteins including α-actinin, cTnT, and Cx43 and increased the tissue contraction under the external electrical stimulation (Fig. 2.2) [76]. There are many investigations using GO as fillers in composites though the conductivity of GO is not so high. For example, a highly elastic hybrid hydrogel composed of methacryloyl-substituted recombinant human tropoelastin (MeTro) and graphene oxide (GO). In this investigation, the features of flexibility, biocompatibility, and ease of dispersion in aqueous solutions for GO were addressed, instead of the conductivity that is compromised due to the oxidation process. The synergistic effect of MeTro and GO significantly enhanced ultimate strain (250%), reversible rotation (9700°), and the fracture energy (38.8 ± 0.8 J/m^2) in the hybrid network. At the same time, the hybrid hydrogels improved electrical signal propagation and subsequent contraction of the muscles connected to some extents in the ex vivo tests [77].

Besides compositing with biological materials, a large number of investigations have reported the integration of graphene with synthetic polymeric materials for cardiac tissue engineering. One example is that the combination of graphene and poly(caprolactone) (PCL) led to the formation of three-dimensional (3D) nanofibrous composite scaffolds for cardiac tissue engineering. It was assumed that the addition of graphene provided local conductive sites within the PCL matrix, which enabled the application of external electrical stimulation throughout the scaffolds. It was observed that mouse embryonic stem cell-derived cardiomyocytes (mES-CM) well adhered on the composite scaffolds and contracted spontaneously and exhibited cardiomyocyte phenotype. Noted that mES-CM cultured on the composite scaffolds exhibited significantly higher fractional release compared to 2D control, and also exhibited a significantly shorter caffeine-induced transient T50 compared to 2D control, all of which indicated that the added graphene especially affected Ca^{2+} handling properties of mES-CM [78]. Another example is a reduced graphene oxide (rGO)-incorporated gelatin methacryloyl (GelMA) hybrid hydrogel. The incorporation of rGO into GelMA hydrogel significantly enhanced the electrical conductivity and mechanical properties of the material. Moreover, cells cultured on the composite hydrogel rGO-GelMA exhibited better biological activities including cell viability, proliferation, and maturation, compared to those cultured on GelMA hydrogels.

Moreover, cardiomyocytes showed stronger contractility and faster spontaneous beating rate on rGO-GelMA sheets compared to those on GelMA sheets [79].

Injection of a conductive hydrogel was designed to provide mechanical support to the infarcted region and synchronize contraction and restore ventricular function by electrically connecting isolated cardiomyocytes to intact tissue. By combining graphene oxide (GO) nanoparticles with oligo(poly(ethylene glycol) fumarate) (OPF), an injectable semiconductive hydrogel was prepared and injected in rats 4 weeks after myocardial infarction. The composite hydrogel OPF/GO provided mechanical support and improved the electric connection between healthy myocardium and the cardiomyocytes in the scar by activating the canonical Wnt signal pathway associating with the generation of Cx43 and gap junction-associated proteins. The Ca^{2+} signal conduction of cardiomyocytes was also enhanced in the infarcted region in comparison with PBS or OPF alone and promoted the generation of cytoskeletal structure and intercalated disc assembly. After 4 weeks of injection, the heart function of load-dependent ejection fraction/fractional shortening was improved [80]. Another example of soft injectable hydrogel with conductive property was produced by incorporating graphene oxide (GO) with a multi-armed crosslinker PEGDA700-Melamine (PEG-MEL), which could crosslink with thiol-modified hyaluronic acid (HA-SH) to form an injectable hydrogel, which exhibited a soft and anti-fatigue mechanical property and conductive property reached to 0.03 S/m. The hydrogel encapsulating adipose tissue-derived stromal cells (ADSCs) was injected into MI area of rats, which significantly increased the expression of α-smooth muscle actin (α-SMA) and connexin 43 (Cx43). Meanwhile a distinct increase of ejection fraction (EF), smaller infarction size, less fibrosis area, and higher vessel density were achieved [81]. By integrating multiple techniques, a group established an approach to fabricate 3D multilayered constructs using layer-by-layer assembly of cardiomyocytes and fibroblasts. In the design, films of GO-containing GelMA gel served as cell adhesive sheets to facilitate the formation of multilayer cell constructs with interlayer connectivity. PLL-modified GO particles were deposited in the first monolayer of the cells grown on the film, followed by the cell adhesion of the second layer. The process was repeated to fabricate the final 3D engineered tissue. This approach might be used to create dense and tightly connected cardiac tissues through the co-culture of cardiomyocytes and other cell types [82].

In addition to the use of fabricating conductive scaffolds, graphene may have potentials in the application of stem cell therapy. An investigation showed that graphene of 0.2 mg/mL embedded into the structure of mouse embryoid bodies (EBs) using hanging drop technique could enhance the mechanical properties and electrical conductivity of the EBs and accelerated the cardiac differentiation of the EB-graphene in the 5-day cultivation, confirmed by high-throughput gene analysis. In addition, electrical stimulation of 4 V and 1 Hz for 10 ms within 2 continuous days further enhanced the cardiac differentiation of the EBs, evidenced by analysis of the cardiac protein and gene expression and the beating activity of the EBs [83]. Like carbon nanotubes, graphene and derivatives are also reported to have the function of ROS scavenging. For example, graphene oxide (GO) flakes could protect the

implanted MSCs from ROS-mediated death and thereby improve the therapeutic efficacy of mesenchymal stem cell (MSC). It is known that MSC implantation is a potential therapy for myocardial infarction (MI). However, the poor survival of the implanted MSCs in the injury sites significantly limited the therapeutic efficacy of this approach, one of the reasons is that reactive oxygen species (ROS) are generated in the ischemic myocardium after the restoration of blood flow, forming a harmful microenvironment to the injected stem cells. This investigation reported that GO significantly prolonged the survival of MSCs due to its clearance ability to ROS and enhanced the paracrine secretion from the MSCs following MSC implantation, which in turn promoted cardiac tissue repair and cardiac function restoration [84].

2.3.2.3 Gold Nanoparticles

Incorporation of electroconductive gold nanoparticles (GNPs) into hydrogels have reported enhancements of myocardial constructs' properties. The advantages are contributed by GNPs not only their metal conductivity and biocompatibility but also the very small size distribution and mechanical reinforcement to the composites in nanoscale. It is not surprising that GNPs can bring conductivity and stiffness to polymeric material poly(2-hydroxyethyl methacrylate) (PHEMA), the resulting Young's moduli of the composites were closer to that of myocardium. Neonatal rat cardiomyocytes exhibited increased expression of connexin 43 on the hybrid scaffolds composed of GNPs and PHEMA, no matter with or without electrical stimulation [85]. A similar example is that hydrogels composed of chitosan (CS) and GNPs were produced with a highly porous network of interconnected pores (CS-GNP). The GNPs of 7 nm in diameter were evenly dispersed throughout the CS matrix to provide electrical and thermal cues. The gelation response and electrical conductivity of the hydrogel were controlled by different concentrations of GNPs, and the conductivity of the CS-GNP hydrogels at the optimal ratio reached 0.13 S/m that was like that of natural heart tissue. The CS-GNP hydrogels supported viability, metabolism, migration, and proliferation of mesenchymal stem cells (MSCs) along with the development of uniform cellular constructs within the 14 days of incubation. Immunohistochemistry for early and mature cardiac markers such as α-MHC and Nkx-2.5 showed enhanced cardiomyogenic differentiation of MSCs within the CS-GNP compared to the CS matrix alone [86]. GNPs were also blended with collagen to form a composite hydrogel. Not addressing the conductivity of the composite hydrogel, researchers focused on the effect of GNPs on topography and the nanoscale local elasticity of scaffolds. They demonstrated that the GNPs increased the hydrogel stiffness locally in nanoscale, which increased the interaction between cardiac myocytes and the substrates, evidenced by the activation of β1-integrin signaling and mediation of the activation of integrin-linked kinase (ILK) and its downstream signal kinase by stimulating the expression of the transcription factors GATA4 and MEF-2c [87]. GNPs could combine with injectable reverse thermal gel (RTG) system that is expected to provide a particularly attractive approach of

being delivered in a minimally invasive manner, thus avoiding mechanical stress on the cells during injection and providing structural support at the injury area. In addition, the injectable hydrogels provide cells encapsulated in three-dimensional (3D) environments; therefore, the hydrogels better mimic the in vivo microenvironment than two-dimensional (2D) cultures. A RTG consisting of poly(serinol hexamethylene urea)-copoly(*N*-isopropylacrylamide) functionalized with lysine was synthesized (RTG-lysine), which conjugated with gold nanoparticles (AuNPs) by free amine groups. The generated RTG-AuNP hydrogel was conductive and could support the survival of neonatal rat ventricular myocytes (NRVMs) for up to 21 days when cocultured with cardiac fibroblasts, the level of connexin 43 (Cx43) for the NRVMs was significantly upregulated in relative to control cultures without AuNPs [88].

Gold nanorods (GNRs) with aspect ratio of 3.15 were reported to be capable of combing with gelatin methacrylate (GelMA) and inducing crosslink among the hydrogel molecules under the irradiation of UV light. The embedded GNRs in hydrogels promoted electrical conductivity and mechanical stiffness of the hydrogel matrix, which properly accommodated cardiac cells and consequently led to excellent cell adhesion, spreading, metabolic activity, homogeneous distribution of cardiac specific markers including sarcomeric α-actinin and connexin 43, cell–cell coupling, as well as robust synchronized beating behavior in the tissue level. In particular, the increased cell adhesion resulted in abundance of locally organized F-actin fibers, leading to the formation of an integrated tissue layer on the GNR-embedded hydrogels. The GelMA-GNR hybrids supported synchronous tissue-level beating of cardiomyocytes in the absence of electrical stimulation and showed good ability for the accommodation of external electrical stimuli, as a significantly lower excitation threshold was gained by the hybrid hydrogels with 1.5 mg/mL of GNRs [89]. It is noticeable that GNRs have been introduced in bioprinting that is one microfabrication method able to create biomimetic three-dimensional (3D) tissue constructs. For example, the composite of gold nanorods (GNRs) and gelatin methacryloyl (GelMA) could be a conductive bioink for printing 3D functional cardiac tissue constructs. An optimal bioink could be prepared by adjusting the concentration of GNRs, which had a low viscosity like pristine inks and allowed rapid deposition of cell-laden fibers at a high resolution, while reducing shear stress on the encapsulated cells. In the printed constructs, cardiac cells showed better adhesion and organization compared to the constructs control without GNRs. The incorporated GNRs bridged the electrically resistant pore walls formed by the polymeric materials (bioink), improving cell-to-cell coupling and promoting synchronized contraction of the bioprinted constructs [90].

Besides blending with macromolecular materials, GNPs can be deposited directly on substrates to play the role of conductivity. It is known that coiled perimysial fibers within the heart muscle can contract and relaxing efficiently. Inspired by the structure of natural coiled perimysial fibers, researchers synthetically fabricated similar coiled electrospun fibers of PCL. The coiled fibers had diameters ranging from a few hundreds of nanometers to several micrometers, and the scaffolds composed with the coiled fibers exhibited an average pore area >4000 μm^2. On the

surface of the fibers, GNPs were evaporated with a nominal thickness of 10 nm to give the fibers conductivity. As a consequence, the composite scaffolds promoted cardiac cell organization into elongated and aligned tissues generating a strong contraction force, high contraction rate and low excitation threshold [91]. This deposition strategy is especially suitable be applied to biological materials that are not able to endure complicated and harsh chemical reactions. For example, GNPs were deposited on fibrous decellularized omental matrices to make the decellularized matrices conductive, which is an attractive design for fabricating engineering functional cardiac patches for treating myocardial infarction. Consequently, the cardiac cells growing within the composite scaffolds exhibited elongated and aligned morphology, massive striation, and organized connexin 43 electrical coupling proteins. The hybrid patches displayed superior function, including a stronger contraction force, lower excitation threshold, and faster calcium transients, as compared to pristine patches [92]. In some cases, GNPs are used with graphene together. A conductive biodegradable scaffold was generated by incorporating graphene oxide gold nanosheets (GO-Au) into a clinically approved natural polymer chitosan (CS). The composite scaffold composed of CS and GO-Au nanosheets displayed two folds increase in electrical conductivity in reference to the chitosan alone scaffold, reaching 0.012 S/m that is 1/10 of that for natural heart tissue. At the same time, the scaffold exhibited excellent porous architecture with desired swelling. In particular, the inclusion of GO-Au reduced the degradation rate of the scaffold because GO-Au sheets hinder the penetration of hydrolytic enzymes inside the polymer matrix that slows down the degradation. In a rat model of MI, the conductive scaffold after 5 weeks of implantation showed a significant improvement in QRS interval, which was associated with enhanced conduction velocity and contractility in the infarct zone by increasing connexin 43 levels [93].

2.3.2.4 Silicon Nanowires

Although silicon nanowires are not well known, they have attractive features of high conductivity and mechanical stiffness, but also biodegradable, and their degradation products are found mainly in the form of $Si(OH)_4$ and are metabolically tolerant in vivo. In one study, n-type SiNWs of 100 nm in diameter and 10 μm in length, and with a ratio of 500 (silane to phosphane) were prepared, the conductivity was as high as150−500 μS/μm, which is much higher than that of cell culture medium (∼1.75 μS/μm) and myocardium (∼0.1 μS/μm). The resulting nanowires were used to improve the differentiation and maturation of human embryonic stem cells (hESC) and human-induced pluripotent stem cells (hiPSC), because current cardiomyocytes derived from hESCs and hiPSCs retain an immature phenotype, including poorly organized sarcomere structures due to the lack of ability for assembling in a controlled manner and led to compromised, unsynchronized contractions. In this study, a trace amount of electrically conductive silicon nanowires (e-SiNWs) was added in scaffold-free cardiac spheroids to create highly electrically conductive microenvironments within spheroids, leading to synchronized and significantly

enhanced contraction, as well as significantly more advanced cellular structural and contractile maturation [94]. In a follow-up study, researchers investigated important factors that could affect functions of hiPSC cardiac spheroids cultured with silicon nanowires, including cell number per spheroid and the electrical conductivity of the silicon nanowires. They explained with a semi-quantitative theory that the two factors were competitive in the improvement of 3D cell–cell adhesion and the reduction of oxygen supply to the center of spheroids with the increase of cell number, and the critical role of electrical conductivity of silicon nanowires was confirmed in improving tissue function of hiPSC cardiac spheroids [95].

2.3.2.5 Mechanistic Exploration of Conductive Scaffolds Enhance Cardiac Tissue Regeneration

Several studies have explored and discussed underlying mechanisms of how conductive scaffolds promote the mechanical integrity and electrophysiological function of cardiac myocytes. For example, single-walled carbon nanotubes were incorporated into collagen or GelMA that was used as growth supports for neonatal cardiomyocytes. Researchers demonstrated that the composite hydrogel enhanced cardiomyocyte adhesion and maturation through β1-integrin-mediated signaling pathway. As is known, a variety of intracellular signaling pathways can be initiated by β1-integrin signaling, including FAK, Src, and ILK, and it was found out that CNTs remarkably accelerated gap junction formation via activation of the β1-integrin-mediated FAK/ERK/GATA4 pathway. In the investigation, a notably higher level of p-FAK was observed in a composite of carbon nanotubes and collagen (CNT-Col) compared to those on collagen alone at all the measured time points, whereas no remarkable changes of p-Src and ILK were noted between two groups, suggesting that FAK was activated and acted as a downstream signaling molecule from β1-integrin. Once FAK is phosphorylated, several downstream signaling kinases can be further activated, including AKT and ERK. Western blotting analysis revealed significant increases in the expression of p-ERK in NRVMs grown on CNT-Col substrates at various developmental phases while no apparent change of p-AKT expression was observed between the two groups, suggesting that ERK was activated by FAK and might be the downstream effector of FAK [96]. It was further demonstrated that the downstream signaling protein RhoA and FAK was responsible for CNT-induced upregulation mechanical junction proteins of NRVMs grown on CNT-GelMA substrates [97].

A recent work compared the effect of mechanical stiffness and nanoscale topography of scaffolds on cell–cell coupling, maturation, and electrical excitability of engineered cardiac tissues. The conductive performance was adjusted by the incorporation of conductive gold nanoparticles or nonconductive silicon nanoparticles. Scaffolds contained silicon nanoparticles. Four different hydrogels were prepared including soft GelMA gel, stiff GelMA gel, GelMA gel containing silicon nanoparticles (nonconductive with nano-topographies and soft), and GelMA gel containing gold nanoparticles (conductive with nano-topographies and stiff). Results highlighted that the influence of nanoscale topography provided by the integrated

nanomaterials was stronger than the elastic modulus and conductivity on cellular adhesion and retention, as well as on the promotion of cardiac cells maturation, suggesting the prominent role of the nanoscale surface topography of nanocomposite scaffolds in the cardiac cell–cell coupling, maturation, and functionalities of the engineered tissue [98]. These results worth of further consideration though they are not consistent with experimental results from nanofibrous scaffolds containing conductive polymers. To gain insights from different views, we fabricated a conductive hydrogel (PVA/CFs) by blending carbon fibers of 7 μm in diameter and PVA that has a simple molecular structure and forms very soft hydrogels [99]. In this composite hydrogel, there were not obvious nanostructures while the carbon fibers are highly conductive with high tensile strength as well as modulus. In addition, the conductive element was carbon, instead of gold. The carbon fibers brought distinguished conductivity of 0.3 S/m and stiffness of 2.3 MPa to the PVA. It was observed that α5 and β1 integrin were both significantly upregulated in neonatal rat cardiomyocytes grown on PVA/CFs compared with those on PVA control, meanwhile the levels of ILK and p-AKT were elevated correspondingly. In addition, hypoxia-inducible factor-1α (HIF-1α) was increased, which was assumed that the cells on PVA/CFs were subjected to a stronger material-support pulling, therefore might experience hypoxia, implying that CFs might provide a microenvironment of promoting angiogenesis in the cells (Fig. 2.3). Noted that these signals are highly

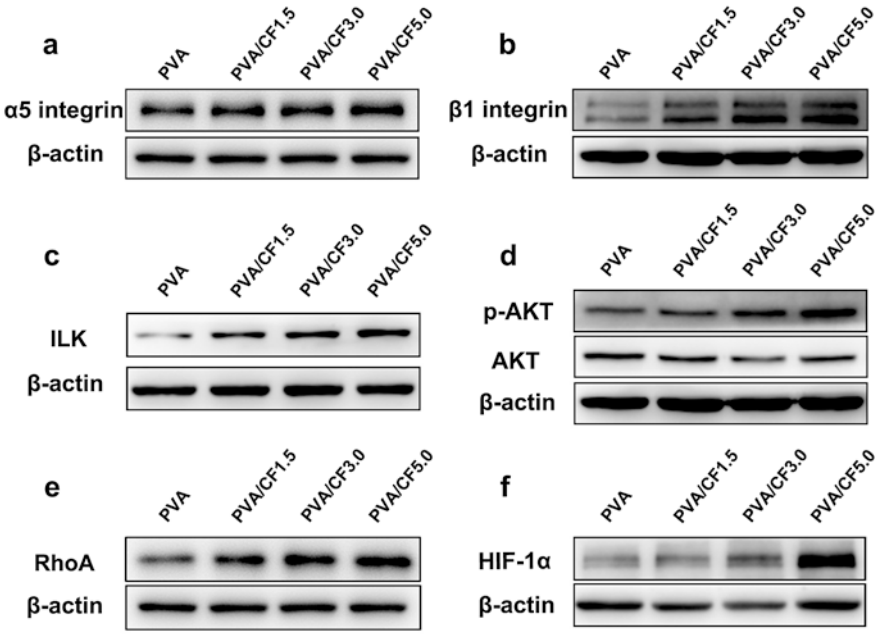

Fig. 2.3 Mechanotransduction signaling is involved in the modulation of CFs with NRCMs. Western blot analysis of the expression of (**a**) α5 integrin, (**b**) β1 integrin, (**c**) ILK, (**d**) p-AKT, (**e**) RhoA, and (**f**) hypoxia-inducible factor 1-α in NRCMs grown on PVA/CFs or PVA alone for 5 days. Data are represented as mean ± standard deviation (SD); $*p < 0.05$, $**p < 0.01$, $***p < 0.001$ by one-way ANOVA analysis [99]

related: AKT can regulate the expression of the gap junction protein Cx43 [100], ILK is a proximal receptor kinase that can regulate integrin-mediated signal transduction and is a key component of sarcomeric contractile apparatus in vertebrate hearts [101], and the integrin-dependent ILK/AKT pathway is involved in the activation of HIF-1α [102]. Besides, RhoA, one of the Rho family members, is also regulated by integrin and plays an important role in regulating the formation and stability of adherent junctions [103], its expression level was also up regulated by PVA/CFs. Therefore, CFs embedded in PVA could enhance cell maturation and tissue regeneration by activating the integrin-mediated mechanotransduction pathway and by accelerating the electrical charges moving. The conductivity and stiffness both are of importance for cardiac tissue engineering scaffolds.

2.4 Conductive Scaffolds for Skeletal and Bone Regeneration

Musculoskeletal system includes skeletal muscle, bone, cartilage, and tendon/ligament, which is one of the main targets for tissue engineering, because there is an increasing need for regeneration and/or repair. Skeletal muscles comprise about 40–45% of an adult human body mass, they are mainly responsible for generating forces which facilitate voluntary movement, postural support, breathing, and locomotion. Skeletal muscle injuries may occur from a variety of events, including direct trauma, such as muscle lacerations, contusions or strains, and indirect causes, such as ischemia, infection, or neurological dysfunction. Even though skeletal muscle cells can naturally regenerate as a response to insignificant tissue damages due to their remarkable robust innate capacity for regeneration, more severe injuries that result in muscle mass loss of more than 20% can cause irreversible loss of muscle cell mass and lead to irreversible fibrosis and scaring. In addition, aging and severe congenital disorders also result in the loss of muscle mass and function. However, so far, cell therapies have not become a good approach to treat those injuries. It has been recognized that electrical stimulation is a very important biophysical cue for skeletal muscle maintenance and myotube formation, for example, the absence of electrical signals from motor neurons can cause denervated muscles to atrophy. Therefore, conductive scaffolds are naturally expected and developed for musculoskeletal system regeneration, since they can mediate electrical stimulation as well as provide cell microenvironments to grow. Moreover, conductive materials usually have capacity of scavenging reactive oxygen species (ROS), which is another advantage that would be beneficial to the protection of cells and tissues.

2.4.1 Carbon-Based Materials Used in Conductive Scaffolds

Carbon nanotubes (CNTs) have been used in skeletal muscle engineering to modulate the conductivity or the mechanical strength of scaffolds toward myotube formation due to their unique mechanical and electrical properties. For example, one

study showed that CNTs can be used directly as substrates for inducing skeletal myogenic differentiation of human mesenchymal stem cells (hMSCs). Because pristine MWCNTs were extremely hydrophobic and rapidly precipitate in aqueous solutions, polyethylene glycol (PEG) was used to modify MWCNTs to increase their hydrophilicity to facilitate scaffold preparation, cell adherence, and growth. The film of PEG-modified MWCNT (PEG-CNT) had nanoscale surface roughness, orderly arrangement, high hydrophilicity, and high mechanical strength [104]. It is noticeable that the films alone could induce the skeletal myogenic differentiation of hMSCs, without any myogenic induction factors. The hMSCs seeded on PEG-CNT films presented significant upregulation of general myogenic markers, including early commitment markers of myoblast differentiation protein-1 (MyoD) and desmin, as well as a late phase marker of myosin heavy chain-2 (MHC), either in the gene level or in the protein level, compared with those on nonconductive control. The gene expression of skeletal muscle-specific marker troponin-C (TnC) and ryanodine receptor-1 (Ryr) was also significantly upregulated in hMSCs on PEG-CNT films. Meanwhile, those cells did not show enhanced adipogenic, chondrogenic, and osteogenic markers. These results suggested the important roles of MWCNTs in the skeletal muscle injury repair. To reduce potential toxicity, multiwalled carbon nanotube (MWCNT) membranes were functionalized by the [4 + 2] Diels–Alder cycloaddition reaction of 1,3-butadiene. In this process, the cycloadducts would disrupt the sp^2 C–C structure into sp^3 geometry at the two neighboring C atoms, weakening but not breaking the C lattice. When subcutaneously implanted in a rat model, the functionalized membranes (p,f-CNTs) induced a slighter intense inflammatory response compared to non-functionalized CNT membranes (p-CNTs), showing a reduced cytotoxicity profile. More important features are that the p,f-CNTs showed in vivo biodegradable property, likely mediated by the oxidation-induced myeloperoxidase (MPO) in neutrophil and macrophage inflammatory milieus. This could potentially avoid long-term tissue accumulation and notable toxicological threats [105].

In many cases, CNTs were taken as fillers in polymeric materials for the fabrication of composite scaffolds. For example, researchers fabricated composite fibers by utilizing carbon nanotubes (CNTs) to enhance the formation of aligned myotubes with improved contractibility of skeletal tissues. The fibers were composed of gelatin and multiwalled carbon nanotubes (MWCNTs) and produced by using electrospinning technique. The aligned fibers were used as scaffolds for the growth of myoblasts (C2C12). It was reported that the incorporated MWCNTs increased the Young's modulus of gelatin but did not improve the bulk fiber conductivity because the concentration of embedded MWCNTs were too low to link to each other, breaking the charge displacement path. Even though, the MWCNTs were considered to possibly generate local conductivity. Experimental results showed that the composite hydrogels enhanced myotube formation by upregulating the expression of mechanotransduction-related genes, and the maturation of the myotubes and the amplitude of the myotube contractions could be further promoted under electrical stimulation [106]. Bone healing can be significantly expedited by applying electrical stimuli in the injured region. An example is to produce randomly oriented and aligned electrically conductive nanofibers of biodegradable poly-DL-lactide (PLA)

by using electrospinning technique, in which MWCNTs were embedded to give conductivity to the fibers. The meshes formed by the conductive fibers offered both topographic cues and electrical stimulation on osteoblasts. In the absence of electrical stimulation, the aligned nanofibers enhanced the extension and directed the outgrowth of osteoblasts better than the random fibers. The cellular elongation and proliferation were mainly dependent on the electrical stimulation. Interestingly, the osteoblasts on all samples grew along the electrical current direction in the presence of direct current (DC) of 100 μA. In this situation, the topographical features played a minor role in them. Therefore, conductive substrate with electrical stimulation was suggested an attractive potential in the application of bone tissue engineering [107].

Graphene and graphene-based composites are emerging rapidly and investigated intensively as conductive materials to fabricate scaffolds for uses in tissue engineering and regenerative medicine. Addition of graphene oxide (GO) nanoplatelets in bioactive polymers was found to enhance the conductivity and dielectric permittivity along with biocompatibility and mechanical properties. A research group prepared thin GO sheets and nanofibrous meshes composed of GO and PCL (GO-PCL) for the cultures of umbilical cord blood (UCB)-derived multipotent mesenchymal stem cells (CB-hMSCs). The GO sheets were dielectric and semiconductive, and the GO-PCL fibrous meshes acquired enhanced conductivity and dielectric permittivity when compared to PCL alone. When CB-hMSCs were seeded, GO-PCL composite was reported to provide more favorable cues to the cells for the formation of superior multinucleated myotubes than the thin GO sheets, enhancing CB-hMSCs differentiate to skeletal muscle cells (hSkMCs) [108]. In another example, nanocomposite materials composed of graphene oxide nanoribbons and hydroxyapatite nanoparticles (nHA) were designed for uses in bone tissue engineering, in which nHA is a bone conductive material and graphene oxide nanoribbons are an electrically conductive material. The composites were detected as nontoxic and enhanced the osteogenesis process compared to controls in a dose-dependent manner, upregulating the expression of ALP, OPN, OCN, COL1, and RUNX2 genes and the secretion of alkaline phosphatase of human osteoblast cell line MG-63. Furthermore, the composites showed higher bone neoformation after 15 days of implantation in a rat tibia defect model and better lamellar bone formation compared to control after 21 days implantation [109]. Similar investigations include following two examples: one is the fabrication of 3D scaffolds composed of graphene and citrate-stabilized hydroxyapatite nanoparticles (nHA) by a facile and universal method that can be used to synthesize such structures based on colloidal chemistry. The resulting gels were reported highly porous, strong, electrically conductive, and biocompatible [110]. The other one is composite scaffolds composed of three kinds of biological materials including alginate, chitosan and collagen, and graphene oxide (GO). The resulting scaffolds had enriched porous structures that were generated by freeze-drying technique, interconnected pores ranging 10–250 μm in diameter. The incorporation of GO increased both crosslinking density and polyelectrolyte ion complex of the polymeric composite, as well as increased mechanical properties. In addition, the GO played a role of stabilizing the porous structures, scaffolds containing GO without chemical crosslinking and was more stable in the aqueous solution compared with the control

scaffolds without GO incorporation. When mouse osteoblast cells were seeded and grown on the scaffolds, cell adhesion was significantly increased [111].

Enthesis is a special complex tissue interface that connects mechanically dissimilar tissues and transfers stress between tendon/ligament and bone. Some sports injuries, such as rotator cuff tendon tear and cruciate ligament rupture, require the reconnection of tendon or ligament to bone. However, these normal critical entheses are not reestablished after repair by surgical techniques; instead, the new connections of tendon or ligament to bone are filled with fibrovascular scar tissue, which would affect the long-term clinical outcome. Therefore, promoting the healing of the bone and tendon/ligament at the implant site is particularly important, and it is surely of significance to develop integrative biomaterials that can facilitate functional tendon to bone integration. It was reported that GO-containing electrospun nanofibrous membranes could provide an effective approach for the regeneration of tendon to bone enthesis. A kind of highly interconnective GO-doped poly(lactide-co-glycolide acid) (GO-PLGA) nanofibrous membrane was fabricated by using electrospinning technique, in which GO was expected to play osteoconductive roles for enhancing tendon/ligament to bone integration. In vitro evaluations demonstrated that GO-PLGA accelerated the proliferation of rabbit bone marrow mesenchymal stem cells (BMSCs) and induced osteogenic differentiation. In a rabbit transosseous supraspinatus tendon repair model, GO-PLGA increased the new bone and cartilage generation in the gap between the tendon and the bone and improved collagen arrangement and biomechanical properties, in comparison with PLGA control, all of which collectively augmented the rotator cuff repairs [112]. For myoblast cells, higher conductivity may be more suitable. The conductivity of graphene oxide (GO) usually lower than pristine graphene because defects are formed during the oxidation process though GO has better dispersibility in aqueous solutions and is more biocompatible than graphene. Reduced GO (rGO) gains increased conductivity compared to that of GO, because the sp^2 carbon bond is partly resorted due to reduction. One study addressed this concern and conducted a mild chemical reduction to graphene oxide/polyacrylamide (GO/PAAm) composite hydrogels to prepare conductive hydrogels r(GO/PAAm), which had electrochemical impedance decreased more than ten times compared to that of GO/PAAm, meanwhile had a Young's modulus of 50 kPa that is similar to the muscle tissue-like stiffness. The r(GO/PAAm) significantly enhanced proliferation and myogenic differentiation compared with GO/PAAm. Moreover, with electrical stimulation, the myogenic gene expression of myoblasts grown on r(GO/PAAm) for 7 days was significantly enhanced compared to unstimulated controls [113].

2.4.2 Conductive Polymers

Conductive polymers are used in the development of scaffolds for skeleton-related tissue regeneration, especially used for skeletal muscle cells of cardiac tissue, possibly due to the requirement of higher conductivity from this specific type of cells.

For example, polyaniline (PANi) was doped with camphorsulfonic acid and blended with poly(glycerol-sebacate) at 10, 20, or 30%, followed by solvent casting to fabricate electrically conductive composite cardiac patches. The electrical conductivity of the composites increased to 0.018 S/cm when PANi content reached 30%. Moreover, the conductivity was preserved for at least 100 h post fabrication, indicating the stability of the composite. At the same time, the elastic modulus, tensile strength, and elasticity were increased as well with the going up of PANi content, and the resulting composites were biocompatible to C2C12 cells [114]. An elastic conductive copolymer (PEGS-AP) was synthesized by grafting aniline pentamer (AP) to poly(ethylene glycol)-co-poly(glycerol sebacate) (PEGS) with an optimal ratio to promote the proliferation and myogenic differentiation of C2C12 cells. The copolymer film showed a proper surface hydrophilicity for cell attachment, conductivity, and mechanical properties. The maximum conductivity of the films reached 0.0184 S/m, and the Young's modulus of these films could range from 14.58 to 24.62 MPa [115].

As it has been mentioned, injectable conductive hydrogels have attracted development interests because they can act as tissue engineering scaffolds and delivery vehicles for electrical signal sensitive cell therapy, especially for myoblast cell therapy and skeletal muscle regeneration. Importantly, the self-healing property can prolong the lifespan of these hydrogels. A kind of self-healable conductive injectable hydrogels was synthesized by using dextran-graft-aniline tetramer-graft-4-formylbenzoic acid and *N*-carboxyethyl chitosan at physiological conditions. The dynamic Schiff base bonds between the formylbenzoic acid and amine group from *N*-carboxyethyl chitosan brought rapid self-healing ability to the hydrogels and biocompatibility as well as the injectability and a linear-like degradation behavior. When mouse myoblasts (C2C12) were encapsulated in the hydrogels by utilizing the self-healing effect, the cells were able to escape from the conductive hydrogels with a linear-like profile, which implied that the hydrogels were potential candidates as cell delivery vehicles and scaffolds for skeletal muscle repair. In the volumetric muscle loss injury model, within the 4 weeks post the implantation, more new muscle tissue formation could be observed at each testing time point in the group of the conductive self-healing than the other control groups [116]. Besides self-healing hydrogels, highly aligned and electrically conductive nanofibers that can simultaneously provide topographical and electrical cues for cells have been reported, which served as functional scaffolds for skeletal muscle tissue engineering. For example, well-ordered nanofibers composed of PANi and poly(ε-caprolactone) (PCL) were produced by using electrospinning technique. The incorporated PANi significantly increased the electrical conductivity of PCL fibers, from a non-detectable level for the pure PCL fibers to 63.6 mS/cm for the fibers containing 3 wt% of PANi. The electrically conductive aligned PCL/PANi nanofibers enhanced myotube maturation compared with nonconductive aligned PCL fibers or random PCL/PANi fibers as well as guided mouse C2C12 myoblasts orientation [117]. Additionally, conductive polymers are considered to have antioxidative effects. For example, a multifunctional material was designed for uses as a coating in porous Ti scaffolds, which was expected to be electroactive, cell affinitive,

persistent ROS-scavenging, and osteoinductive. A composite film composed of polypyrrole, polydopamine, and hydroxyapatite (PPY-PDA-HA) was fabricated in situ synthesized and uniformly coated on a porous scaffold from inside to outside by utilizing a layer-by-layer pulse electrodeposition (LBL-PED) method. In this design, there were PPY-PDA nanoparticles (NPs) and HA NPs in the coating, aiming for bring conductivity and osteoconductivity, respectively. The content of PDA was expected to enhance the ROS scavenging rate of the scaffold within a long period, the content of HA and electrical stimulation synergistically promote osteogenic cell differentiation films [118]. Piezoelectric materials are also important candidates in the application of skeletal tissue regeneration. For example, piezoelectric polymer poly(vinylidene fluoride) (PVDF) can present physical cues to muscle cells that mimic the natural regeneration environment to improve muscle regeneration, because it is able to induce transient surface charge boosting cell growth and differentiation compared with non-piezoelectric controls. One group investigated how the surface properties of the material, in terms of both the charge state and the morphology, influenced myoblast differentiation. They observed enhanced myogenic differentiation of C2C12 cells grown on PVDF by quantitative examination of myotube fusion, maturation index, length, diameter, and number. It is interesting to see that charged surfaces improved the fusion of muscle cells into differentiated myotubes, while the fiber orientation generated influence upon the cell morphology; contrary to the randomly oriented fibers, oriented PVDF electrospun fibers promoted the alignment of the cells [119]. Besides being used in scaffolds for skeletal muscle cells of cardiac tissue, there are investigations of utilizing conductive polymers in bone tissue engineering. As one example, therefore, a three-dimensional (3D) ceramic conductive tissue engineering scaffold for large bone defects was prepared by employing a biocompatible conductive polymer, poly(3,4-ethylenedioxythiophene) poly(4-styrene sulfonate) (PEDOT:PSS), in the optimized nanocomposite of gelatin and bioactive glass. The resulting composite scaffold enhanced the viability of adult human mesenchymal stem cells; meanwhile, the incorporation of PEDOT:PSS increased the physiochemical stability of the composite, resulting in improved mechanical properties and biodegradation resistance. These results suggested that conductive bioactive glass could be produced, which would be structurally more favorable for bone tissue engineering, and may by combined with tissue engineering techniques to enhance bone healing by electrical stimuli [120].

2.5 Conductive Materials for Nerve Regeneration and Treatment

The peripheral nervous system (PNS) is capable of regeneration in adult mammals. Immediately after injury, the tip of the proximal stump swells to two or three times its original diameter and the severed axons retract. Several days later, the proximal

axons begin to sprout vigorously, and growth cones emerge to elicit numerous extensions that extend outward in all directions until the first sprout reaches an appropriate target. In successful regeneration, axons sprouting from the proximal nerve stump traverse the injury site, enter the distal nerve stump, and make new connections with target organs. The most severe injury is a complete transaction of the nerve, interrupting communication between the nerve cell body and its target, disrupts the interrelations between neurons and their support cells, destroys the local blood–nerve barrier, and triggers a variety of cellular and humoral events. Although current surgical techniques allow surgeons to realign nerve ends precisely when the lesion does not require excision of a large nerve segment. However, damages in large scale depend on nerve guidance channels to help the regeneration process, because the rate of axon elongation is as low as 1 mm per day in average in humans. When a nerve guidance channel is used, the mobilized ends of a severed nerve are introduced in the lumen of a tube and anchored in place with sutures. The channel can provide a path between nerve stumps, directional guidance for elongation neurites and migrating cells, proximal-distal stump communication, and minimal number of epineurial stay sutures, prevent scar tissue invasion into the regenerating environment, and preserve endogenous trophic or growth factors released by the traumatized nerve ends within the channel lumen. In addition, guidance channels are useful to experimental studies, for example, control the gap distance between the nerve stumps, examine the fluid and tissue entering the channel, modulate the physicochemical properties of the channel, and apply various drugs, gels, and Shawn cells in channels to investigate the regulatory effects [121]. Technologies in the fabrication of tissue engineering scaffolds provide more choices for conventional nerve conduits, especially that to introduce conductive materials and nanostructures into scaffolds. Advances in the past decade have showed that conductive scaffolds by utilizing nanotechnology and conductive materials promoted neuronal proliferation and differentiation by providing an environment around nerve tissue of electrical signal exchange and conduction properties.

2.5.1 Conductive Polymers

In an early study, an electrospun scaffold (PANI/PG) was prepared by blending doped polyaniline (PANi) in the mixed solution of poly (epsilon-caprolactone) and gelatin in a ratio of 70:30 solution, followed by processed with electrospinning technique. The nanofibrous scaffolds containing 15% PANi showed the most balanced properties to meet the required specifications for electrical stimulation and were suitable for the attachment and proliferation of nerve stem cells. When an electrical stimulation was directly applied, both cell proliferation and neurite outgrowth were enhanced compared to the PANI/PG scaffolds that were not subjected to electrical stimulation [122]. When blended with polyethyleneglycol diacrylate (PEGDA), PANi brought conductivity to the macroporous hydrogels crosslinked

via UV irradiation, 1.1×10^{-3} mS/cm with 3 wt% of PANi and improved the biological response of rat pheochromocytoma 12 (PC12) and hMSC cells. The hydrophilic nature of PANi also enhanced water retention and proton conductivity by more than one order of magnitude [123]. Polypyrrole (PPY) is also a good candidate for being used as a conductive component in scaffolds of nerve engineering. In one study, a conducting nerve conduit composed of PPY and poly(D, L-lactic acid) (PDLLA) was fabricated, and the PPY content of PPY 5%, 10%, and 15% resulted in the conductivity 5.65, 10.40, and 15.56 mS/cm, respectively. When PC12 cells were seeded on these conduits and stimulated with 100 mV for 2 h, there was a marked increase in both the percentage of neurite-bearing cells and the median neurite length in a PPY concentration-dependent manner. More encouragingly, when the PPY/PDLLA nerve conduit was used to repair a rat sciatic nerve defect, it performed similarly to the gold standard autologous graft in the 6-month investigation. In particular, the PPY/PDLLA conduit started degradation at the 3-month post implantation when the 10 mm gap was bridged by regenerative tissue [124]. Another form of three-dimensional PPY conductive fibrous scaffold was fabricated by using electrospinning technique to produce PLLA fibers and have PPY coated on the fiber surface with a thickness of 45 nm. The average diameter of the PPY-coated PLLA fibers was 2.1 μm. The size of interconnected pores in the scaffolds ranged from 50 to 100 μm. This conductive 3D scaffold was superior to the conductive fibrous mesh, which ensured cells entry into inside of the scaffolds to achieve three-dimensional cell culture. It was reported that more PC12 cells were detected in the 3D scaffolds than that on the fibrous meshes in the 3 days culture and developed cell–fiber constructs in the central of conductive 3D scaffolds [125]. In some situations, mechanical properties of scaffolds are addressed, that the mechanical performance would be better close to that of the corresponding natural tissue. For example, it is considered that it is crucial to mimic mechanical properties and high conductivities of soft tissues in the design for nerve tissue regeneration scaffolds, as that are required for electrical transmission in the native spinal cord. For example, a soft, highly conductive hydrogel was prepared by using a plant-derived polyphenol, tannic acid (TA), and conducting polypyrrole (PPY) for guiding tissue regeneration after a spinal cord injury. The hydrogel obtained electrical conductivity of 0.05–0.18 S/cm and mechanical property of 0.3–2.2 kPa, which was controlled by TA concentration. The increased conductivity of the scaffolds accelerated the differentiation of neural stem cells into neurons while suppressing the development of astrocytes and, more importantly, activated the neurogenesis of endogenous neural stem cells in the lesion area to recover the locomotor function [126]. As mentioned before, Schwann cells play important roles in the nerve regeneration as they are the supportive cells to the neuronal cells. The myelination of Schwann cells is crucial for the success of peripheral nerve regeneration, and scaffolds promoting Schwann cells to secret neurotrophin would be beneficial for nerve repair. An investigation reported a highly tunable conductive biodegradable flexible polyurethane by polycondensation of poly(glycerol sebacate) and aniline pentamer, which significantly enhanced Schwann cells' myelin gene expression and neurotrophin secretion. The mechanism of Schwann cells' neurotrophin secretion on conductive films is

attributed to the increase of intracellular Ca^{2+} level. The enhanced Schwann cells' myelin gene expressions and sustained neurotrophin secretion would be of potential for nerve regeneration [127].

2.5.2 Inorganic Nanoparticles

The utilization of conductive nanomaterials as fillers in various polymeric materials is one important and effective solution to develop neural tissue engineering scaffolds. As one of the conductive nanomaterials, graphene has huge potentials in nerve function restoration by promoting electrical signal transduction and metabolic activities with unique topological properties. The underlying mechanisms are involved with the interface interaction between graphene and neural cell membrane. A mechanistic study indicated that graphene did not affect the basic membrane electrical parameters of neural stem cells, the electric field produced by the electronegative cell membrane was much higher on graphene substrates than that on control, which indicated that graphene was able to accelerate neural stem cell maturation during development, especially with regard to bioelectric evolvement [128]. It was reported that reduced GO (rGO) nanosheets could be integrated with porcine acellular dermal matrix (PADM) mainly composed of type I collagen to prepare a porous 3D, biodegradable, conductive, and biocompatible PADM-rGO hybrid. The rGO in the scaffold did not induce a significant change in the microstructure but endowed the PADM-rGO composite with good conductivity. Rat bone-marrow-derived mesenchymal stem cells (MSCs) cultured on PADM-rGO composite showed a higher level of neural markers including Nestin, Tuj1, GFAP, and MAP2, both in protein and gene level, after 7 days under neural differentiation conditions than those on PADM alone, suggesting that the PADM-rGO promoted the differentiation of MSCs into neuronal cells as well as support the growth of MSCs at a high proliferation rate [129]. It is well known that polydopamine (PDA) and arginylglycylaspartic acid (RGD) can improve cell adhesion in tissue engineering. A study combined the technology of 3D printing and layer-by-layer casting (LBLC) to fabricate a multilayered porous scaffold composed of multilayered graphene (MG) coated with PDA/RGD and polycaprolactone (PCL). The conductive 3D graphene scaffold significantly improved neural expression both in vitro and in vivo, promoting successful axonal regrowth and remyelination after peripheral nerve injury [130]. The rGO-based composite can also act as a medium for step-driven TENG pulse electrical simulation signals in the nerve regeneration. Currently almost all electrical stimulation for clinical or experimental nerve regeneration is supplied by traditional electrical stimulators using a 220 V power supply, which are considered expensive, not portable, and need an external power supply however may with safety risk. Battery-like power suppliers may have problems such as low-voltage, short duration, and difficult to adhere to the animal models of patients. To meet the needs, a group established a long-lasting and portable self-powered electrical stimulation system by combining reduced graphene oxide (rGO) and a conductive

polymer poly(3,4-ethylenedioxythiophene) (PEDOT). The highly electrically conductive composite (rGO-PEDOT) microfiber with a diameter of 80 μm was prepared as neural scaffolds. A step-driven self-powered neural differentiation system was integrated by combining the composite microfiber and a TENG system [131] with outputs of 250 V and 30 μA. The rGO-PEDOT composite microfiber could not only enhance the proliferation of MSCs but also act as a medium for step-driven TENG pulse electrical simulation signals, inducing MSCs to differentiate into neural cells. This approach showed the application potentials of a self-powered wearable TENG electrical stimulation system to assist nerve regeneration for a walking person [132].

Carbon nanotubes are another typical conductive nanomaterial easily to be combined with various polymeric materials to generate conductive composites. One example is the integration of carbon nanotube fibers (CNFs) with polysaccharide agarose to prepare conductive hydrogels for neural tissue engineering and biointerfacing with the nervous system. The CNFs can be chemically functionalized by agarose to gain biological moieties. The agarose-modified CNF was reported conductive and nontoxic and could facilitate cell attachment and response both in vitro and in vivo [133]. As another example, multiwalled carbon nanotubes (MWCNTs) were combined with poly(lactic-co-glycolic acid) (PLGA) to generate electrically conductive and aligned nanofibrous scaffolds for nerve regeneration. The surface was modified with poly-L-lysine to provide a better environment for cell attachment. The aligned conductive fibers were reported to guide PC12 cells and dorsal root ganglion (DRG) neurons growing along the fiber direction and be beneficial for neurite outgrowth. Moreover, PC12 cells and DRG neurons stimulated with electrical shock of 40 mV showed longer neurite length. In this study, the cell attachment, proliferation, and MBP expression of Schwann cells were also enhanced with the synergistic effect of aligned nanofibers and electrical stimulation [134]. Carbon nanotubes could be combined with plasma-treated chitin to generate composite scaffolds for neuron repair/regeneration. The addition of carbon nanotubes to the chitin biopolymer improved the electrical conductivity and the assisted oxygen plasma treatment introduced more oxygen species onto the scaffold surface, which in turn increased neuron adhesion as well as maintained synaptic function of neurons [135]. To promote the differentiation of human neural stem/progenitor cells (hNSPCs), single-walled carbon nanotubes (SWCNTs) were introduced with polypyrrole (PPY) together into hyaluronic acid (HA) hydrogel by the oxidative catechol chemistry used for hydrogel cross-linking. The prepared electroconductive HA hydrogels were reported to be dynamic, electrically conductive, and biocompatible, significantly promoted neuronal differentiation of human fetal neural stem cells (hfNSCs) and human-induced pluripotent stem cell-derived neural progenitor cells (hiPSC-NPCs) with improved electrophysiological functionality when compared to the control HA hydrogel, as shown that calcium channel expression was upregulated, depolarization was activated, and intracellular calcium influx was increased in hNSPCs that were differentiated in 3D electroconductive HA-CA hydrogels [136]. In neural injury, potassium chloride cotransporter 2 (KCC2) was repressed, which plays a co-contributory role by corrupting inhibitory neurotransmission. It was

detected that highly conductive few-walled-CNT (fwCNT) had influence on primary CNS neurons originating from the cerebral cortex, inducing Cl− downregulation and KCC2 upregulation, which made the chloride shift robustly and strikingly accelerated. This effect was demonstrated specific for fwCNT since SiOx nanowires (a nanomaterial with similar nanostructure yet not conductive) did not affect the chloride shift. The result is of implications to the development of novel devices that interface with nervous tissues [137].

2.6 Wound Healing

Serious injuries resulted from trauma, burns, and clinical surgery would severely affect one's life and health. Wound repair and tissue regeneration are complex processes that bring challenges in the development of wound dressings with potent biological activity and physiological signal response ability to accelerate the process of wound healing. There is a large need of wound dressing for seriously injured skin wound in clinical practices, because skin is the largest organ in human body protecting the body from damage and bacterial infection and maintaining body fluid, electrolytes, and nutritional component.

It is known that skin is an electrical signal-sensitive tissue; the conductivity values can be from 1×10^{-4} mS/cm to 2.6 mS/cm, depending on skin components [138]; therefore, induction of conductive materials in skin wound dressing would be beneficial to the skin regeneration. In addition, when a wound dressing gains a certain degree of conductivity, it would hold an ability of free radical scavenging, which is likely to benefit to tissue regeneration possibly by reducing proinflammatory substances.

For example, a conductive self-healing and injectable hydrogel fabricated by using two polymeric materials formed a crosslinking network: one is quaternized chitosan grafted with polyaniline and the other is benzaldehyde group functionalized poly(ethylene glycol)-co-poly(glycerol sebacate) (PEGS-FA). The conductivity of the resulting hydrogel was 0.23–0.35 S/m. Noted that the hydrogel showed free radical scavenging ability, biocompatibility, and intrinsic antibacterial activity that was attributable to chitosan. Interestingly, the hydrogel with an optimal formulation showed excellent in vivo blood clotting capacity, and it significantly enhanced in vivo wound healing process in a full-thickness skin defect model than the control of nonconductive hydrogel and commercial dressing control. At the same time, the hydrogel increased the gene expression level of growth factors including VEGF, EGF, and TGF-β in the regenerated skin tissue, and the granulation tissue thickness and collagen deposition were promoted. These results indicated the important contribution of the conductivity of the hydrogel among the multifunctional properties [138]. Similar multifunctional hydrogels were designed by mixing the biocompatible *N*-carboxyethyl chitosan (CEC) and oxidized hyaluronic acid-graft-aniline tetramer (OHA-AT) under physiological conditions. The hydrogels exhibited stable rheological property, high swelling ratio, suitable gelation time, good in vitro

biodegradation property, electroactive property, and free radical scavenging capacity. The antibacterial activity of this hydrogel was contributed by the addition of antibiotic amoxicillin, effectively preventing the wound infection. In vivo experiments indicated that hydrogel with aniline tetramer addition significantly accelerated wound healing rate with higher granulation tissue thickness, collagen disposition, and more angiogenesis in a full-thickness skin defect model, suggesting the conductive component made main contribution to the tissue regeneration instead of the antibacterial property [139].

Besides polymeric conductive components, potentials of inorganic nanomaterials have also been investigated in conductive wound dressing. Carbon nanomaterials have become attractive to wound dressing mainly due to the excellent biocompatibility of carbon materials, for example, carbon materials have been used as coatings in various kinds of blood-contacting medical devices [140], as well as their conductivity. Carbon nanotubes are one typical carbon-based nanomaterials and have been demonstrated excellent blood compatibility when in the form of non-woven membrane [141] or to improve biocompatibility of polyurethane when embedded in the polymeric matrix [142, 143]. We have reported that electrospun nanofibrous membranes composed of multiwalled carbon nanotubes (MWCNTs) and polyurethane (PU) showed friend interactions to fibroblast cells that are major supportive cells in skin. The MWCNTs increased the content of pure carbon to improve the biocompatibility and conductivity of the nanofibrous membrane. Interestingly, the composite nanofibrous membrane displayed stronger function of supporting cell adhesion and proliferation than the control membrane without MWCNTs. In particular, the composite membrane enhanced cell–cell connection compared with the control membrane, and fibroblasts grown on the composite nanofibrous membrane formed cell sheets (Fig. 2.4), suggesting the membrane provided a favorite environment for the fibroblasts to migrate and communicate. Furthermore, the cells growing on the nanofibrous composite membrane released the biological signals to the population growing on the smooth film of PU to encourage the population's proliferation [144]. In addition, single-walled carbon nanotube non-woven films could be used directly as scaffolds to support fibroblast cell growth for long-term proliferation [145].

Reduced graphene is another kind of conductive carbon nanomaterial explored in wound healing dressings; it also has strong adsorption capacity to various biological molecules as well as high conductivity. Researchers developed a polydopamine (PDA)-reduced graphene oxide (pGO) that was then dispersed into a mixture of chitosan (CS) and silk fibroin (SF) (CS/SF), aiming to acquire adhesive property and conductivity at the same time. In the resulting hydrogel, pGO was considered as nanoreinforcement to enhance the mechanical properties of the scaffold and comprised a well-connected electric pathway to provide a channel for the transmission of electrical signals in the scaffold. Moreover, pGO could scavenge reactive oxygen species (ROS) to inhibit excessive ROS oxidation. Due to these collective properties, the electroactive pGO-CS/SF scaffolds could respond to electrical signals and enhance the wound healing in full-thickness skin defect model [146]. A similar design of adhesive hemostatic antioxidant conductive photothermal antibacterial

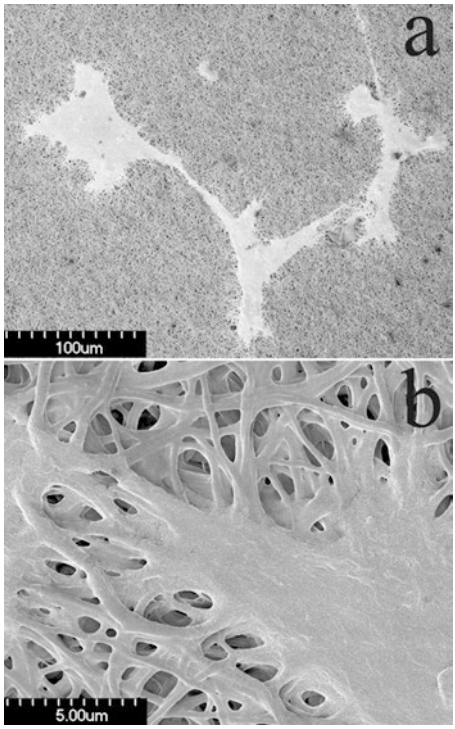

Fig. 2.4 Morphological observation of cells growing on nanofibrous scaffold of MWNT/PU under SEM, in which (**a**) exhibited the cell sheets and cell "chains" formed on nanofibrous scaffold of MWNT/PU; (**b**) SEM image with higher magnification showed the cells spread and integrated well with the nanofibrous scaffold of MWNT/PU [144]

hydrogels was reported, and the hydrogel was composed of hyaluronic acid-graft-dopamine and reduced graphene oxide, having high swelling, degradability, tunable rheological property, and similar mechanical properties to human skin. It had been noted that the hydrogel dressings significantly enhanced vascularization by upregulating growth factor expression of CD31 and improved the granulation tissue thickness and collagen deposition to promote wound closure in a mouse full-thickness wounds model [147].

Hemorrhage control is an important issue of wound healing, not only in military and civilian trauma centers, but also in clinics. Uncontrolled hemorrhage leads to over 30% of trauma deaths in the world, and more than 50% of those occur before the emergency care can reach. Hence, hemostatic agents that can quickly control massive hemorrhage from vessels and visceral organs are highly needed, however have remain challenged. A research group designed an injectable antibacterial conductive cryogels by integrating carbon nanotubes (CNTs) and glycidyl methacrylate functionalized quaternized chitosan for uses in lethal noncompressible hemostasis and wound healing (Fig. 2.5). It is noticeable that the CNT content varying from 2 to 4 and 6 mg/mL resulted in the increase of conductivity for the cryogels, increasing from 0.04 to 0.095 and 0.12 S/m, respectively, showing the obvious contribution of CNT to the cryogels' conductivity. These cryogels were reported to have better blood-clotting ability and higher blood cell and platelet adhesion and activation than gelatin sponge and gauze in mouse liver injury model and mouse tail amputation

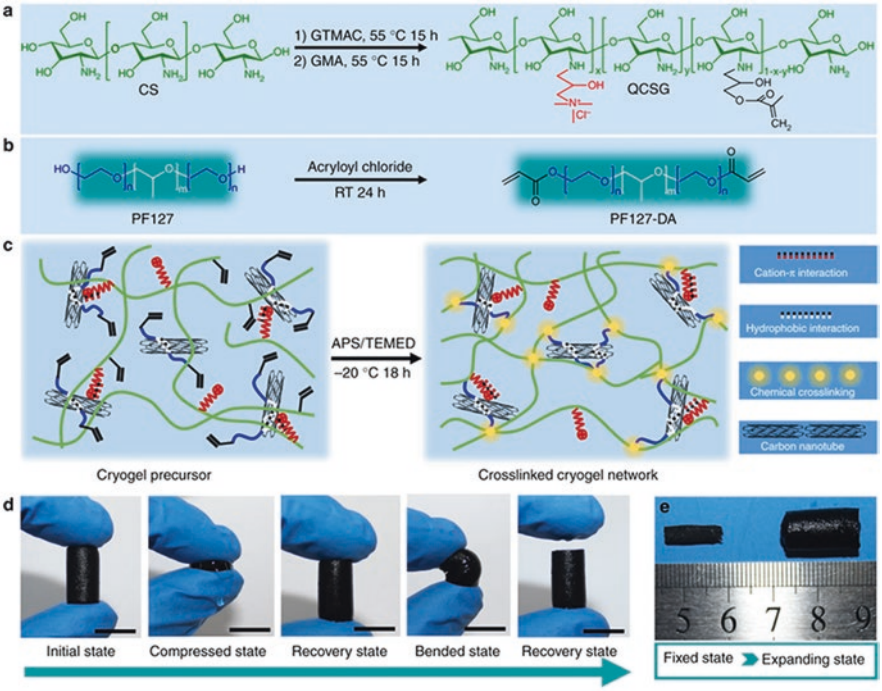

Fig. 2.5 Injectable antibacterial conductive nanocomposite cryogels with rapid shape recovery for noncompressible hemorrhage and wound healing. Schematic representation of QCSG/CNT cryogel synthesis. (**a**) Synthesis of QCSG copolymer. GTMAC and GMA with a fixed 0.5:1 molar ratio of GMA to amino groups and varying the GTMAC:amino groups from 1:1 (coded as QCSG1) to 2:1 (coded as QCSG2) and 3:1 (coded as QCSG3). (**b**) Synthesis of PF127-DA copolymer. (**c**) Preparation of QCSG/CNT cryogel. (**d**) Photographs of the compression and bending resistance capability of QCSG/CNT4 cryogels: initial state, compressed state by squeezing out of the free water, recovery state by absorbing water, bending, and squeezing out of part free water, and recovery state after absorbing water. (**e**) Shape-fixed state after removing the free water (left) and expanding state after absorbing water (right). Scale bar: 1 cm [148]

model (Fig. 2.6), and excellent hemostatic performance in rabbit liver defect lethal noncompressible hemorrhage model [148]. Here one issue could be discussed that in this investigation, the rapid clotting was mainly attributed to the chitosan component, and the CNT was considered to trigger the platelet activation as well. We would like to address that whether CNTs play anticoagulant roles (hemocompatibility) or play hemostatic performance is highly dependent on the application way of CNTs, that is, the way of contacting blood. It has been demonstrated that the carbon nanotubes integrated with polyurethane improved the blood compatibility of the composite [143] or showed excellent performance of inhibiting the activation of platelets when in the form of nonwoven membrane [141]. However, when carbon nanotubes were dispersed in buffer saline, they exhibited the effect of inducing blood coagulation [149]. It could be noted that the CNTs in the hydrogel for

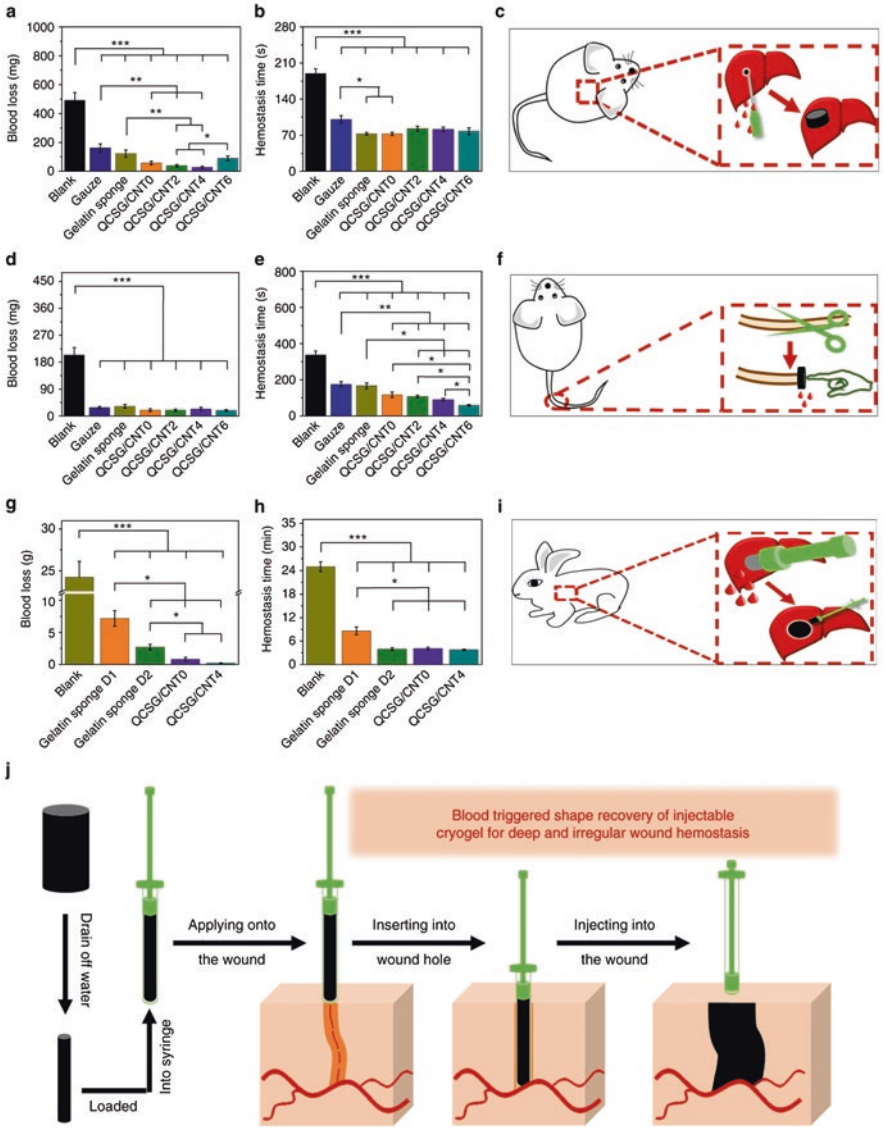

Fig. 2.6 Injectable antibacterial conductive nanocomposite cryogels with rapid shape recovery for noncompressible hemorrhage and wound healing. In vivo hemostatic capacity evaluation of the cryogels. Blood loss (**a**) and hemostatic time (**b**) in the mouse liver injury model. The blank group showed the highest blood loss of 492 mg than the other groups ($P < 0.001$). Gauze and gelatin sponge, as two control groups, presented much decreased blood loss of about 163 and 123 mg, respectively, when compared to blank group ($P < 0.001$). However, all the four cryogels except for QCSG/CNT6 showed significantly decreased blood loss of 57, 38, and 27 mg than those of gauze, and the cryogel QCSG/CNT2 and cryogel QCSG/CNT4 also showed significantly decreased blood loss than that of gelatin sponge ($P < 0.05$). (**c**) Scheme representation of the mouse liver injury model during hemostasis. Blood loss (**d**) and hemostatic time (**e**) in the mouse tail amputation

hemostasis might contact platelets in a status of dispersing nanoparticles when the hydrogel was injected in liver, because there is a large amount of water in the hydrogel. In this case, the CNTs could trigger platelet activation to a certain extent. Differently, when carbon nanotubes were integrated with polymeric materials, they combined with polymer chains tightly, therefore exhibiting the performance of macroscale carbon materials.

2.7 Perspectives

Large numbers of investigations have showed that conductive materials are of great significance to tissue engineering and regenerative medicine, they have remarkable impacts on important events of cell growth, differentiation, and formation of new tissues with physiological functions by creating electrically active microenvironments mimicking natural physiological conditions. The conductive scaffolds with or without electrical stimulations have been applied to excitable tissues such as cardiac and skeletal and nerve and also bone and skin, therefore exhibiting promising potentials in the repair of tissue defects and injury as well as in creating tissue in vitro. Nevertheless, challenges are existing, including improvements of conductive polymers' stability and biocompatibility and long-term safety of conductive nanomaterials. Moreover, it is necessary to have the measurements for conductivity of different scaffolds standardized and data comparable in the future, which would be helpful to design novel conductive scaffolds that are available to be controlled precisely.

References

1. F.A. Duck, *Physical Properties of Tissues: A Comprehensive Reference Book* (Academic, San Diego, 2013)
2. R. Balint, N.J. Cassidy, S.H. Cartmell, Conductive polymers: towards a smart biomaterial for tissue engineering. Acta Biomater. **10**(6), 2341–2353 (2014)
3. J.H. Min, M. Patel, W.G. Koh, Incorporation of conductive materials into hydrogels for tissue engineering applications. Polymers (Basel) **10**(10) (2018). pii: E1078

Fig. 2.6 (continued) model. The blank group (337 s) showed the longest hemostatic time than other groups ($P < 0.001$). All the four cryogels showed shorter hemostatic times than gauze group (176 s) ($P < 0.01$), while all the four cryogels except for QCSG/CNT0 showed shorter hemostatic times than gelatin sponge group (167 s) ($P < 0.05$). (**f**) Schematic representation of the mouse tail amputation model during hemostasis; Blood loss (**g**) and hemostatic time (**h**) in the rabbit liver defect lethal noncompressible hemorrhage model. (**i**) Scheme representation of the rabbit liver defect lethal noncompressible hemorrhage model during hemostasis. (**j**) Schematic representation of the hemostatic application of injectable shape memory cryogel hemostatic in a deep and irregularly shaped wound model. $*P < 0.05$, $**P < 0.01$, $***P < 0.001$ using Student's *t*-test (two-sided). The error bars stand for SEM ($n = 10$ for **a**, **b**, **d**, **e**; $n = 5$ for **g**, **h**) [148]

4. M. Potse, B. Dube, A. Vinet, Cardiac anisotropy in boundary-element models for the electrocardiogram. Med. Biol. Eng. Comput. **47**(7), 719–729 (2009)
5. A.K. Geim, K.S. Novoselov, The rise of graphene. Nat. Mater. **6**(3), 183–191 (2007)
6. C. Chung et al., Biomedical applications of graphene and graphene oxide. Acc. Chem. Res. **46**(10), 2211–2224 (2013)
7. S. Park, R.S. Ruoff, Chemical methods for the production of graphenes. Nat. Nanotechnol. **4**(4), 217–224 (2009)
8. Y. Zhu et al., Graphene and graphene oxide: synthesis, properties, and applications. Adv. Mater. **22**(35), 3906–3924 (2010)
9. K.S. Novoselov et al., A roadmap for graphene. Nature **490**(7419), 192–200 (2012)
10. D. Li, R.B. Kaner, Graphene-based materials. Science **320**(5880), 1170–1171 (2008)
11. H. Dai, Carbon nanotubes: opportunities and challenges. Surf. Sci. **500**(1-3), 218–241 (2002)
12. J.M. Schnorr, T.M. Swager, Emerging applications of carbon nanotubes. Chem. Mater. **23**(3), 646–657 (2010)
13. V.N. Popov, Carbon nanotubes: properties and application. Mater. Sci. Eng. R Rep. **43**(3), 61–102 (2004)
14. I. Sumio, Carbon nanotubes: past, present, and future. Phys. B Condens. Matter. **323**(1–4), 1–5 (2002)
15. P.R. Bandaru, Electrical properties and applications of carbon nanotube structures. J. Nanosci. Nanotechnol. **7**(4–5), 1239–1267 (2007)
16. H. Dai, Carbon nanotubes: synthesis, integration, and properties. Acc. Chem. Res. **35**(12), 1035–1044 (2002)
17. R.H. Baughman, A.A. Zakhidov, W.A. de Heer, Carbon nanotubesDOUBLEHYPHENthe route toward applications. Science **297**(5582), 787–792 (2002)
18. M. Shao, D.D.D. Ma, S.-T. Lee, Silicon nanowires – synthesis, properties, and applications. Eur. J. Inorg. Chem. **2010**(27), 4264–4278 (2010)
19. Y. Wu et al., Controlled growth and structures of molecular-scale silicon nanowires. Nano Lett. **4**(3), 433–436 (2004)
20. P.R. Bandaru, P. Pichanusakorn, An outline of the synthesis and properties of silicon nanowires. Semicond. Sci. Technol. **25**(2), 024003 (2010)
21. V. Schmidt, J.V. Wittemann, U. Gösele, Growth, thermodynamics, and electrical properties of silicon nanowires. Chem. Rev. **110**(1), 361–388 (2010)
22. L.J. Chen, Silicon nanowires: the key building block for future electronic devices. J. Mater. Chem. **17**(44), 4639–4643 (2007)
23. R. Rurali, Colloquium: structural, electronic and transport properties of silicon nanowires. Rev. Mod. Phys. **82**(1), 427–449 (2010)
24. Y. Zheng et al., Electronic properties of silicon nanowires. IEEE Trans. Electron Devices **52**(6), 1097–1103 (2005)
25. D.A. Giljohann et al., Gold nanoparticles for biology and medicine. Angew. Chem. Int. Ed. **49**(19), 3280–3294 (2010)
26. X. Zhang, Gold nanoparticles: recent advances in the biomedical applications. Cell Biochem. Biophys. **72**(3), 771–775 (2015)
27. H.-H. Jeong et al., Recent advances in gold nanoparticles for biomedical applications: from hybrid structures to multi-functionality. J. Mater. Chem. B **7**(22), 3480–3496 (2019)
28. J. Siegel et al., Properties of gold nanostructures sputtered on glass. Nanoscale Res. Lett. **6**(1), 96 (2011)
29. E.C. Dreaden et al., The golden age: gold nanoparticles for biomedicine. Chem. Soc. Rev. **41**(7), 2740–2779 (2012)
30. R. Sardar et al., Gold nanoparticles: past, present, and future. Langmuir **25**(24), 13840–13851 (2009)
31. R.A. Sperling et al., Biological applications of gold nanoparticles. Chem. Soc. Rev. **37**(9), 1896–1908 (2008)
32. S. Alex, A. Tiwari, Functionalized gold nanoparticles: synthesis, properties and applicationsDOUBLEHYPHENa review. J. Nanosci. Nanotechnol. **15**(3), 1869–1894 (2015)

33. G. Schmid, U. Simon, Gold nanoparticles: assembly and electrical properties in 1–3 dimensions. Chem. Commun. **6**, 697–710 (2005)
34. A.B. Afzal et al., Investigation of structural and electrical properties of polyaniline/gold nanocomposites. J. Phys. Chem. C **113**(40), 17560–17565 (2009)
35. M. Ahamed, M.S. Alsalhi, M.K. Siddiqui, Silver nanoparticle applications and human health. Clin. Chim. Acta **411**(23–24), 1841–1848 (2010)
36. X.F. Zhang et al., Silver nanoparticles: synthesis, characterization, properties, applications, and therapeutic approaches. Int. J. Mol. Sci. **17**(9), 1534 (2016)
37. J. Meng et al., Using gold nanorods core/silver shell nanostructures as model material to probe biodistribution and toxic effects of silver nanoparticles in mice. Nanotoxicology **8**(6), 686–696 (2014)
38. H. Guo et al., Intravenous administration of silver nanoparticles causes organ toxicity through intracellular ROS-related loss of inter-endothelial junction. Part. Fibre Toxicol. **13**, 21 (2016)
39. H. Li et al., In vivo metabolic response upon exposure to gold nanorod core/silver shell nanostructures: modulation of inflammation and upregulation of dopamine. Int. J. Mol. Sci. **21**(2) (2020). pii: E384
40. B. Wiley, Y. Sun, Y. Xia, Synthesis of silver nanostructures with controlled shapes and properties. Acc. Chem. Res. **40**(10), 1067–1076 (2007)
41. D. Chen et al., Synthesis and electrical properties of uniform silver nanoparticles for electronic applications. J. Mater. Sci. **44**(4), 1076–1081 (2009)
42. S.M. Adhyapak, V.R. Parachuri, Architecture of the left ventricle: insights for optimal surgical ventricular restoration. Heart Fail. Rev. **15**(1), 73–83 (2010)
43. R. Hashizume et al., Biodegradable elastic patch plasty ameliorates left ventricular adverse remodeling after ischemia–reperfusion injury: a preclinical study of a porous polyurethane material in a porcine model. J. Thorac. Cardiovasc. Surg. **146**(2), 391–399.e1 (2013)
44. D.D. Ateh, H.A. Navsaria, P. Vadgama, Polypyrrole-based conducting polymers and interactions with biological tissues. J. R. Soc. Interface **3**(11), 741–752 (2006)
45. X. Liu et al., Conducting polymers with immobilised fibrillar collagen for enhanced neural interfacing. Biomaterials **32**(30), 7309–7317 (2011)
46. A. Mihic et al., A conductive polymer hydrogel supports cell electrical signaling and improves cardiac function after implantation into myocardial infarct. Circulation **132**(8), 772–784 (2015)
47. Z. Cui et al., Polypyrrole-chitosan conductive biomaterial synchronizes cardiomyocyte contraction and improves myocardial electrical impulse propagation. Theranostics **8**(10), 2752–2764 (2018)
48. S. He et al., Preservation of conductive propagation after surgical repair of cardiac defects with a bio-engineered conductive patch. J. Heart Lung Transplant. **37**(7), 912–924 (2018)
49. A. Gelmi et al., Direct mechanical stimulation of stem cells: a beating electromechanically active scaffold for cardiac tissue engineering. Adv. Healthc. Mater. **5**(12), 1471–1480 (2016)
50. G. Kaur et al., Electrically conductive polymers and composites for biomedical applications. RSC Adv. **5**(47), 37553–37567 (2015)
51. Y. He et al., Mussel-inspired conductive nanofibrous membranes repair myocardial infarction by enhancing cardiac function and revascularization. Theranostics **8**(18), 5159–5177 (2018)
52. J.H. Tsui et al., Conductive silk–polypyrrole composite scaffolds with bioinspired nanotopographic cues for cardiac tissue engineering. J. Mater. Chem. B **6**(44), 7185–7196 (2018)
53. P.R. Bidez III et al., Polyaniline, an electroactive polymer, supports adhesion and proliferation of cardiac myoblasts. J. Biomater. Sci. Polym. Ed. **17**(1-2), 199–212 (2006)
54. M. Li et al., Electrospinning polyaniline-contained gelatin nanofibers for tissue engineering applications. Biomaterials **27**(13), 2705–2715 (2006)
55. C.-W. Hsiao et al., Electrical coupling of isolated cardiomyocyte clusters grown on aligned conductive nanofibrous meshes for their synchronized beating. Biomaterials **34**(4), 1063–1072 (2013)

56. L. Wang et al., Electrospun conductive nanofibrous scaffolds for engineering cardiac tissue and 3D bioactuators. Acta Biomater. **59**, 68–81 (2017)
57. M. Kapnisi et al., Auxetic cardiac patches with tunable mechanical and conductive properties toward treating myocardial infarction. Adv. Funct. Mater. **28**(21), 1800618 (2018)
58. P.T. Bertuoli et al., Electrospun conducting and biocompatible uniaxial and core-shell fibers having poly(lactic acid), poly(ethylene glycol), and polyaniline for cardiac tissue engineering. ACS Omega **4**(2), 3660–3672 (2019)
59. X. Zhao et al., Antibacterial and conductive injectable hydrogels based on quaternized chitosan-graft-polyaniline/oxidized dextran for tissue engineering. Acta Biomater. **26**, 236–248 (2015)
60. B. Yang et al., Development of electrically conductive double-network hydrogels via one-step facile strategy for cardiac tissue engineering. Adv. Healthc. Mater. **5**(4), 474–488 (2016)
61. J. Zhou et al., Engineering the heart: evaluation of conductive nanomaterials for improving implant integration and cardiac function. Sci. Rep. **4**(1), 3733 (2014)
62. S. Pok et al., Biocompatible carbon nanotube-chitosan scaffold matching the electrical conductivity of the heart. ACS Nano **8**(10), 9822–9832 (2014)
63. B. Peña et al., Injectable carbon nanotube-functionalized reverse thermal gel promotes cardiomyocytes survival and maturation. ACS Appl. Mater. Interfaces **9**(37), 31645–31656 (2017)
64. S. Ahadian et al., Moldable elastomeric polyester-carbon nanotube scaffolds for cardiac tissue engineering. Acta Biomater. **52**, 81–91 (2017)
65. M. Kharaziha et al., Tough and flexible CNT–polymeric hybrid scaffolds for engineering cardiac constructs. Biomaterials **35**(26), 7346–7354 (2014)
66. N. Shokraei et al., Development of electrically conductive hybrid nanofibers based on CNT-polyurethane nanocomposite for cardiac tissue engineering. Microsc. Res. Tech. **82**(8), 1316–1325 (2019)
67. J. Meng et al., Electrospun aligned nanofibrous composite of MWCNT/polyurethane to enhance vascular endothelium cells proliferation and function. J. Biomed. Mater. Res. A **95A**(1), 312–320 (2010)
68. Y. Wu et al., Interwoven aligned conductive nanofiber yarn/hydrogel composite scaffolds for engineered 3D cardiac anisotropy. ACS Nano **11**(6), 5646–5659 (2017)
69. J. Ren et al., Superaligned carbon nanotubes guide oriented cell growth and promote electrophysiological homogeneity for synthetic cardiac tissues. Adv. Mater. **29**(44) (2017). https://doi.org/10.1002/adma.201702713
70. S.R. Shin et al., Carbon-nanotube-embedded hydrogel sheets for engineering cardiac constructs and bioactuators. ACS Nano **7**(3), 2369–2380 (2013)
71. X. Li et al., A PNIPAAm-based thermosensitive hydrogel containing SWCNTs for stem cell transplantation in myocardial repair. Biomaterials **35**(22), 5679–5688 (2014)
72. J. Wang et al., Graphene sheet-induced global maturation of cardiomyocytes derived from human induced pluripotent stem cells. ACS Appl. Mater. Interfaces **9**(31), 25929–25940 (2017)
73. A.S.T. Smith et al., Micro- and nano-patterned conductive graphene–PEG hybrid scaffolds for cardiac tissue engineering. Chem. Commun. **53**(53), 7412–7415 (2017)
74. A.J. Ryan et al., Electroconductive biohybrid collagen/pristine graphene composite biomaterials with enhanced biological activity. Adv. Mater. **30**(15), e1706442 (2018)
75. M.H. Norahan et al., Electroactive graphene oxide-incorporated collagen assisting vascularization for cardiac tissue engineering. J. Biomed. Mater. Res. A **107**(1), 204–219 (2019)
76. G. Zhao et al., Reduced graphene oxide functionalized nanofibrous silk fibroin matrices for engineering excitable tissues. NPG Asia Mater. **10**(10), 982–994 (2018)
77. N. Annabi et al., Highly elastic and conductive human-based protein hybrid hydrogels. Adv. Mater. **28**, 40–49 (2016)
78. P. Hitscherich et al., Electroactive graphene composite scaffolds for cardiac tissue engineering. J. Biomed. Mater. Res. A **106**(11), 2923–2933 (2018)
79. S.R. Shin et al., Reduced graphene oxide-GelMA hybrid hydrogels as scaffolds for cardiac tissue engineering. Small **12**(27), 3677–3689 (2016)

80. J. Zhou et al., Injectable OPF/graphene oxide hydrogels provide mechanical support and enhance cell electrical signaling after implantation into myocardial infarct. Theranostics **8**(12), 3317–3330 (2018)
81. R. Bao et al., A π-π conjugation-containing soft and conductive injectable polymer hydrogel highly efficiently rebuilds cardiac function after myocardial infarction. Biomaterials **122**, 63–71 (2017)
82. S.R. Shin et al., Layer-by-layer assembly of 3D tissue constructs with functionalized graphene. Adv. Funct. Mater. **24**(39), 6136–6144 (2014)
83. S. Ahadian et al., Graphene induces spontaneous cardiac differentiation in embryoid bodies. Nanoscale **8**(13), 7075–7084 (2016)
84. J. Park et al., Graphene oxide flakes as a cellular adhesive: prevention of reactive oxygen species mediated death of implanted cells for cardiac repair. ACS Nano **9**(5), 4987–4999 (2015)
85. J.-O. You et al., Nanoengineering the heart: conductive scaffolds enhance Connexin 43 expression. Nano Lett. **11**(9), 3643–3648 (2011)
86. P. Baei et al., Electrically conductive gold nanoparticle-chitosan thermosensitive hydrogels for cardiac tissue engineering. Mater. Sci. Eng. C **63**, 131–141 (2016)
87. Y. Li et al., AuNP-collagen matrix with localized stiffness for cardiac-tissue engineering: enhancing the assembly of intercalated discs by beta1-integrin-mediated signaling. Adv. Mater. **28**(46), 10230–10235 (2016)
88. B. Peña et al., Gold nanoparticle-functionalized reverse thermal gel for tissue engineering applications. ACS Appl. Mater. Interfaces **11**(20), 18671–18680 (2019)
89. A. Navaei et al., Gold nanorod-incorporated gelatin-based conductive hydrogels for engineering cardiac tissue constructs. Acta Biomater. **41**, 133–146 (2016)
90. K. Zhu et al., Gold nanocomposite bioink for printing 3D cardiac constructs. Adv. Funct. Mater. **27**(12) (2017). pii: 1605352
91. S. Fleischer et al., Coiled fiber scaffolds embedded with gold nanoparticles improve the performance of engineered cardiac tissues. Nanoscale **6**(16), 9410–9414 (2014)
92. M. Shevach et al., Gold nanoparticle-decellularized matrix hybrids for cardiac tissue engineering. Nano Lett. **14**(10), 5792–5796 (2014)
93. S. Saravanan et al., Graphene oxide-gold nanosheets containing chitosan scaffold improves ventricular contractility and function after implantation into infarcted heart. Sci. Rep. **8**(1), 15069 (2018)
94. Y. Tan et al., Silicon nanowire-induced maturation of cardiomyocytes derived from human induced pluripotent stem cells. Nano Lett. **15**(5), 2765–2772 (2015)
95. Y. Tan et al., Cell number per spheroid and electrical conductivity of nanowires influence the function of silicon nanowired human cardiac spheroids. Acta Biomater. **51**, 495–504 (2017)
96. H. Sun et al., Carbon nanotubes enhance intercalated disc assembly in cardiac myocytes via the β1-integrin-mediated signaling pathway. Biomaterials **55**, 84–95 (2015)
97. H. Sun et al., Carbon nanotube-composite hydrogels promote intercalated disc assembly in engineered cardiac tissues through β1-integrin mediated FAK and RhoA pathway. Acta Biomater. **48**, 88–99 (2017)
98. A. Navaei et al., The influence of electrically conductive and non-conductive nanocomposite scaffolds on the maturation and excitability of engineered cardiac tissues. Biomater. Sci. **7**(2), 585–595 (2019)
99. F. Wu et al., High modulus conductive hydrogels enhance in vitro maturation and contractile function of primary cardiomyocytes for uses in drug screening. Adv. Healthc. Mater. **7**(24), e1800990 (2018)
100. C.A. Dunn, P.D. Lampe, Injury-triggered Akt phosphorylation of Cx43: a ZO-1-driven molecular switch that regulates gap junction size. J. Cell Sci. **127**(2), 455–464 (2014)
101. G. Bendig et al., Integrin-linked kinase, a novel component of the cardiac mechanical stretch sensor, controls contractility in the zebrafish heart. Genes Dev. **20**(17), 2361–2372 (2006)
102. C.H. Tang et al., Ultrasound induces hypoxia-inducible factor-1 activation and inducible nitric-oxide synthase expression through the integrin/integrin-linked kinase/Akt/mammalian target of rapamycin pathway in osteoblasts. J. Biol. Chem. **282**(35), 25406–25415 (2007)

103. S.J. Zhang, G.A. Truskey, W.E. Kraus, Effect of cyclic stretch on β1D-integrin expression and activation of FAK and RhoA. Am. J. Physiol. Cell Physiol. **292**(6), C2057–C2069 (2007)
104. C. Zhao et al., Spontaneous and specific myogenic differentiation of human mesenchymal stem cells on polyethylene glycol-linked multi-walled carbon nanotube films for skeletal muscle engineering. Nanoscale **7**(43), 18239–18249 (2015)
105. D. Mata et al., Diels–Alder functionalized carbon nanotubes for bone tissue engineering: in vitro/in vivo biocompatibility and biodegradability. Nanoscale **7**(20), 9238–9251 (2015)
106. S. Ostrovidov et al., Myotube formation on gelatin nanofibers – multi-walled carbon nanotubes hybrid scaffolds. Biomaterials **35**(24), 6268–6277 (2014)
107. S. Shao et al., Osteoblast function on electrically conductive electrospun PLA/MWCNTs nanofibers. Biomaterials **32**(11), 2821–2833 (2011)
108. B. Chaudhuri et al., Myoblast differentiation of human mesenchymal stem cells on graphene oxide and electrospun graphene oxide-polymer composite fibrous meshes: importance of graphene oxide conductivity and dielectric constant on their biocompatibility. Biofabrication **7**(1), 015009 (2015)
109. J.S. Medeiros et al., Nanohydroxyapatite/graphene nanoribbons nanocomposites induce in vitro osteogenesis and promote in vivo bone neoformation. ACS Biomater Sci. Eng. **4**, 1580–1590 (2018)
110. X. Xie et al., Graphene and hydroxyapatite self-assemble into homogeneous, free standing nanocomposite hydrogels for bone tissue engineering. Nanoscale **7**(17), 7992–8002 (2015)
111. E. Kolanthai et al., Graphene oxide—a tool for the preparation of chemically crosslinking free alginate–chitosan–collagen scaffolds for bone tissue engineering. ACS Appl. Mater. Interfaces **10**(15), 12441–12452 (2018)
112. W. Su et al., Promoting tendon to bone integration using graphene oxide-doped electrospun poly(lactic-co-glycolic acid) nanofibrous membrane. Int. J. Nanomedicine **14**, 1835–1847 (2019)
113. H. Jo et al., Electrically conductive graphene/polyacrylamide hydrogels produced by mild chemical reduction for enhanced myoblast growth and differentiation. Acta Biomater. **48**, 100–109 (2017)
114. T.H. Qazi et al., Development and characterization of novel electrically conductive PANI–PGS composites for cardiac tissue engineering applications. Acta Biomater. **10**(6), 2434–2445 (2014)
115. R. Dong et al., Biocompatible elastic conductive films significantly enhanced myogenic differentiation of myoblast for skeletal muscle regeneration. Biomacromolecules **18**(9), 2808–2819 (2017)
116. B. Guo et al., Degradable conductive self-healing hydrogels based on dextran-graft-tetraaniline and N-carboxyethyl chitosan as injectable carriers for myoblast cell therapy and muscle regeneration. Acta Biomater. **84**, 180–193 (2019)
117. M.-C. Chen, Y.-C. Sun, Y.-H. Chen, Electrically conductive nanofibers with highly oriented structures and their potential application in skeletal muscle tissue engineering. Acta Biomater. **9**(3), 5562–5572 (2013)
118. T. Zhou et al., A mussel-inspired persistent ROS-scavenging, electroactive, and osteoinductive scaffold based on electrochemical-driven in situ nanoassembly. Small **15**(25), e1805440 (2019)
119. S. Ribeiro et al., Electroactive biomaterial surface engineering effects on muscle cells differentiation. Korean J. Couns. Psychother. **92**, 868–874 (2018)
120. A. Shahini et al., 3D conductive nanocomposite scaffold for bone tissue engineering. Int. J. Nanomedicine **9**, 167–181 (2014)
121. J.D. Bronzino, *Biomedical engineering Handbook* (CRC Press, Boca Raton, 2000)
122. L. Ghasemi-Mobarakeh et al., Electrical stimulation of nerve cells using conductive nanofibrous scaffolds for nerve tissue engineering. Tissue Eng. Part A **15**(11), 3605–3619 (2009)
123. V. Guarino et al., Conductive PANi/PEGDA macroporous hydrogels for nerve regeneration. Adv. Healthc. Mater. **2**(1), 218–227 (2013)

124. H. Xu et al., Conductive PPY/PDLLA conduit for peripheral nerve regeneration. Biomaterials **35**(1), 225–235 (2014)
125. L. Jin et al., A novel fluffy conductive polypyrrole nano-layer coated PLLA fibrous scaffold for nerve tissue engineering. J. Biomed. Nanotechnol. **8**(5), 779–785 (2012)
126. L. Zhou et al., Soft conducting polymer hydrogels cross-linked and doped by tannic acid for spinal cord injury repair. ACS Nano **12**(11), 10957–10967 (2018)
127. Y. Wu et al., Electroactive biodegradable polyurethane significantly enhanced Schwann cells myelin gene expression and neurotrophin secretion for peripheral nerve tissue engineering. Biomaterials **87**, 18–31 (2016)
128. R. Guo et al., Accelerating bioelectric functional development of neural stem cells by graphene coupling: Implications for neural interfacing with conductive materials. Biomaterials **106**, 193–204 (2016)
129. W. Guo et al., Construction of a 3D rGO-collagen hybrid scaffold for enhancement of the neural differentiation of mesenchymal stem cells. Nanoscale **8**(4), 1897–1904 (2016)
130. Y. Qian et al., An integrated multi-layer 3D-fabrication of PDA/RGD coated graphene loaded PCL nanoscaffold for peripheral nerve restoration. Nat. Commun. **9**(1), 323 (2018)
131. Q. Zheng et al., Biodegradable triboelectric nanogenerator as a life-time designed implantable power source. Sci. Adv. **2**(3), e1501478 (2016)
132. W. Guo et al., Self-powered electrical stimulation for enhancing neural differentiation of mesenchymal stem cells on graphene-poly(3,4-ethylenedioxythiophene) hybrid microfibers. ACS Nano **10**(5), 5086–5095 (2016)
133. D.Y. Lewitus et al., Biohybrid carbon nanotube/agarose fibers for neural tissue engineering. Adv. Funct. Mater. **21**(14), 2624–2632 (2011)
134. J. Wang et al., The cellular response of nerve cells on poly-l-lysine coated PLGA-MWCNTs aligned nanofibers under electrical stimulation. Korean J. Couns. Psychother. **91**, 715–726 (2018)
135. N. Singh et al., Chitin and carbon nanotube composites as biocompatible scaffolds for neuron growth. Nanoscale **8**(15), 8288–8299 (2016)
136. J. Shin et al., Three-dimensional electroconductive hyaluronic acid hydrogels incorporated with carbon nanotubes and polypyrrole by catechol-mediated dispersion enhance neurogenesis of human neural stem cells. Biomacromolecules **18**(10), 3060–3072 (2017)
137. W. Liedtke et al., Highly conductive carbon nanotube matrix accelerates developmental chloride extrusion in central nervous system neurons by increased expression of chloride transporter KCC2. Small **9**(7), 1066–1075 (2013)
138. X. Zhao et al., Antibacterial anti-oxidant electroactive injectable hydrogel as self-healing wound dressing with hemostasis and adhesiveness for cutaneous wound healing. Biomaterials **122**, 34–47 (2017)
139. J. Qu et al., Degradable conductive injectable hydrogels as novel antibacterial, anti-oxidant wound dressings for wound healing. Chem. Eng. J. **362**, 548–560 (2019)
140. L. Feng, J.D. Andrade, Protein adsorption on low temperature isotropic carbon: V. How is it related to its blood compatibility? J. Biomater. Sci. Polym. Ed. **7**(5), 439–452 (1995)
141. J. Meng et al., Effects of single-walled carbon nanotubes on the functions of plasma proteins and potentials in vascular prostheses. Nanomedicine **1**(2), 136–142 (2005)
142. J. Meng et al., Preparation and biocompatibility evaluation of polyurethane filled with multiwalled carbon nanotubes. J. Nanosci. Nanotechnol. **13**(2), 1467–1471 (2013)
143. J. Meng et al., Improving the blood compatibility of polyurethane using carbon nanotubes as fillers and its implications to cardiovascular surgery. J. Biomed. Mater. Res. A **74**(2), 208–214 (2005)
144. J. Meng et al., Enhancement of nanofibrous scaffold of multiwalled carbon nanotubes/polyurethane composite to the fibroblasts growth and biosynthesis. J. Biomed. Mater. Res. A **88**(1), 105–116 (2009)
145. J. Meng et al., Using single-walled carbon nanotubes nonwoven films as scaffolds to enhance long-term cell proliferation in vitro. J. Biomed. Mater. Res. A **79**(2), 298–306 (2006)

146. P. Tang et al., Mussel-inspired electroactive and antioxidative scaffolds with incorporation of polydopamine-reduced graphene oxide for enhancing skin wound healing. ACS Appl. Mater. Interfaces **11**(8), 7703–7714 (2019)
147. Y. Liang et al., Adhesive hemostatic conducting injectable composite hydrogels with sustained drug release and photothermal antibacterial activity to promote full-thickness skin regeneration during wound healing. Small **15**(12), 1900046 (2019)
148. X. Zhao et al., Injectable antibacterial conductive nanocomposite cryogels with rapid shape recovery for noncompressible hemorrhage and wound healing. Nat. Commun. **9**(1), 2784 (2018)
149. J. Meng et al., Effects of long and short carboxylated or aminated multiwalled carbon nanotubes on blood coagulation. PLoS One **7**(7), e38995 (2012)